ABSTRACT

MECHANICAL PROPERTIES AND STRESS-STRAIN BEHAVIOR OF HIGH PERFORMANCE CONCRETE UNDER UNIAXIAL COMPRESSION

by
Pornchai Jiratatprasot

Many recent innovations in advanced concrete materials technology have made it possible to produce concrete with exceptional performance characteristics. High performance concrete (HPC) is defined as concrete that meets special performance and uniformity requirements that cannot always be achieved routinely by using conventional materials and normal mixing, placing, and curing practices. The importance of HPC to structural engineering is unquestionable. However, HPC is a relatively new material. Some results of research on conventional concrete are not entirely applicable. In this experiment, the main mechanical properties of HPC including compressive strength, modulus of elasticity, and Poisson's ratio were investigated and compared to those of normal strength concrete (NSC). The stress-strain behavior under uniaxial and cyclic compression as well as cracking characteristics of HPC were also observed in this research and compared to the existing results from the former researchers.

According to the test results of HPC in this experiment, compressive strength was the one that was most spectacularly improved. The modulus of elasticity was also increased, which could be observed from the steeper slope of the ascending part of the stress-strain curve. Poisson's ratio of HPC was found to be lower than that of NSC, which means HPC experiences less lateral deformation than NSC when it is subjected to the same level of loading. It can be seen in the studies of stress-strain behavior for both types of concrete that HPC has a lower ductility ratio than that of NSC. For this reason, it

can be concluded that HPC has less capability to sustain large inelastic deformation without substantial reduction in strength. This capability can be improved by using steel reinforcements, mostly in the form of lateral confinements such as in columns. When the results of stress-strain curves were compared to the existing models, it was found that the existing models could be applied to the experimental data. Cracking in HPC was observed to be more localized; the number and length of continuous crack patterns developed at failure are smaller than those of NSC. For this reason, the failure mode of HPC cylinders is typical of that of nearly homogeneous material. Finally, HPC showed less amount of hysteresis under cyclic loading. It can be concluded that HPC has less capability to dissipate energy under loading than that of NSC. HPC also showed less stiffness degradation under unloading and reloading cycles than that of NSC, especially in the post-peak regime.

MECHANICAL PROPERTIES AND STRESS-STRAIN BEHAVIOR OF HIGH PERFORMANCE CONCRETE UNDER UNIAXIAL COMPRESSION

by
Pornchai Jiratatprasot

A Thesis
Submitted to the Faculty of
New Jersey Institute of Technology
in Partial Fulfillment of the Requirements for the Degree of
Master of Science in Civil Engineering

Department of Civil and Environmental Engineering

January 2002

APPROVAL PAGE

MECHANICAL PROPERTIES AND STRESS-STRAIN BEHAVIOR OF HIGH PERFORMANCE CONCRETE UNDER UNIAXIAL COMPRESSION

Pornchai Jiratatprasot

Dr. Methi Wecharatana, Thesis Advisor — Date
Professor of Civil and Environmental Engineering, NJIT

Dr. Cheng-Tzu Thomas Hsu, Committee Member — Date
Professor of Civil and Environmental Engineering, NJIT

Dr. Ala Saadeghvaziri, Committee Member — Date
Professor of Civil and Environmental Engineering, NJIT

BIOGRAPHICAL SKETCH

Author: Pornchai Jiratatprasot

Degree: Master of Science

Date: January 2002

Undergraduate and Graduate Education:

- Master of Science in Civil Engineering,
  New Jersey Institute of Technology, Newark, NJ, 2002

- Bachelor of Engineering in Civil Engineering,
  Chulalongkorn University, Bangkok, Thailand, 1998

Major: Civil Engineering

To my beloved family

ACKNOWLEDGMENT

I would like to express my sincere gratitude to my research supervisor, Dr. Methi Wecharatana for his valuable guidance and moral support throughout this research. Special thanks are given to Dr. Cheng-Tzu Thomas Hsu and Dr. Ala Saadeghvaziri for actively participating in my committee.

I would also like to thank Mr. Allyn Luke and all my friends for helping out in every possible way to prepare and run the experiments.

Finally, I am very grateful to the Department of Civil and Environmental Engineering of NJIT for their financial support during my studies at NJIT.

TABLE OF CONTENTS

TABLE OF CONTENTS
(Continued)

LIST OF TABLES

LIST OF FIGURES

LIST OF FIGURES
(Continued)

Figure **Page**

CHAPTER 1

INTRODUCTION

1.1 General

1.1.1 Historical Background

Concrete construction was already known to the Romans, and possibly also to other ancient peoples, but apparently it later fell into disuse. Although the Romans made cement called *pozzolana* by mixing slaked lime with a volcanic ash from Mount Vesuvius and used it to make concrete for building, the arts were lost during the Dark Ages and were not revived until the eighteenth and nineteenth centuries. A deposit of natural cement rock was discovered in England in 1796 and was sold as "Roman cement." Various other deposits of natural cement were discovered in both Europe and America and were used for several decades.

The real breakthrough for concrete occurred in 1824 when an English bricklayer named Joseph Aspdin, after long and laborious experiments, obtained a patent for a cement which he called "portland cement" because its color was quite similar to that of the stone quarried on the Isle of Portland off the English coast. He made his cement by taking certain quantities of clay and limestone, pulverizing them, burning them in his kitchen stove, and grinding the resulting clinker into a fine powder. During the early years after its development, his cement was primarily used in stuccos. This wonderful product was very slowly adopted by the building industry and was not even introduced into the United States until 1868. The first portland cement was not manufactured in the United States until the 1870s [20].

Most of concrete usage is in the form of reinforced concrete. The beginnings of reinforced concrete go back to 1850, when Lambot constructed a small boat of cement which was shown at the World Fair in Paris, 1855, and is still floating in the Parc de Miraval. In England, W.B. Wilkinson patented a true reinforced concrete floor slab in 1854. Seven years later, F. Coignet published his statement on the principles of the new construction, defining the principles of reinforced concrete and describing the proposed construction of girders, vaults, and pipes. He exhibited these structures at the Exhibition of 1867. In 1861, J. Moneir, a Paris gardener, used metal frames as reinforcement for garden tubs and pots. In the same year he took out his first patents [22].

In the United States, the pioneering efforts were made by Thaddeus Hyatt, originally a lawyer, who conducted experiments on reinforced concrete beams in 1850s. In a perfectly correct manner the iron bars in Hyatt's beams were located in tension zone, bent up near the supports, and anchored in the compression zone. Additionally, transverse reinforcement (known as vertical stirrups) was used near the supports. However, Hyatt's experiments were unknown until 1877 when he published his work privately. As head of the Concrete-Steel Company of San Francisco, E.L. Ransome apparently used some form of reinforced concrete in the early 1870s. He continued to increase the application of wire rope and hoop iron to many structures and was the first person to use and have patented in 1884; the deformed (twisted) bar.

The Moneir German patents were sold to G.A. Wayss and Company of Germany in 1880. Tests of structural strength were conducted by German engineers during the 1880s. Theories and computational methods were published by Koenen and Wayss in 1886. Test results of Wayss and J. Bauschinger were published in 1887 [10].

Hennebique developed the construction of reinforced concrete in the direction of *monolithic continuity* of the various structural members, which, up to the present time, has remained one of the principle characteristics of this construction. He also introduced the T-beam in reinforced concrete construction with transverse reinforcement of the web by stirrups [22].

In 1890, Ransome built the Leland Stanford Jr. Museum in San Francisco; a reinforced concrete building two stories high and 312 ft (95 m) long. Since that time, development of reinforced concrete in the United States has been rapid. During the period 1891-1894, various investigators in Europe published theories and test results; among them were Moeller (Germany), Wunsch (Hungary), Melan (Austria), Hennebique (France), and Emperger (Hungary), but practical use was less extensive than in the United States.

Throughout the entire period 1850-1900, relatively little was published, as the engineers working in the reinforced concrete field considered construction and computational methods as trade secrets. One of the first publications that might be classified as a textbook was that of Considere in 1899. By the turn of the century, there was a multiplicity of systems and methods with little uniformity in design procedures, allowable stresses, and system of reinforcing. In 1903, with the formation of the United States of joint committee of representatives of all organizations interested in reinforced concrete, uniform application of knowledge to design was initiated.

In the first decade of the twentieth century, progress in reinforced concrete was rapid. Extensive testing to determine beam behavior, compressive strength of concrete, and modulus of elasticity was conducted by A.N. Talbot at the University of Illinois, by

F.E. Turneaure and M.O. Withey at the University of Wisconsin, and by Bach in Germany, among others. From about 1916 to the mid-1930s, research centered on axially loaded column behavior. In the late 1930s and 1940s, eccentrically loaded columns, footings, and the ultimate strength of beams received special attention.

During the 1950s, emphasis was given to the study of prestressed concrete, and in the 1960s, to strength as a design criterion, particularly with regard to shear-related failures in concrete beams. Parameters affecting shear strength have been studied, with considerable attention focused on torsional strength, including its interaction with bending moment and shear. The behavior of various types of slab floor systems has been experimentally studied, particularly with regard to strength and cracking. Earthquake resistance of structures, including behavior of shear walls, has received and is continuing to attract wide attention. More knowledge about the structural behavior of reinforced concrete has probably been obtained since 1950 than in all previous years combined [10].

1.1.2 Advantages and Disadvantages of Using Concrete as a Structural Material

Reinforced concrete may be the most important material available for construction. It is used in one form or another for almost all structures, big or small buildings, bridges, pavements, dams, retaining walls, tunnels, viaducts, drainage and irrigation facilities, tanks, and so on.

The tremendous success of this universal construction material can be understood quite easily if its numerous advantages are considered. These include the following:

1. It has considerable compressive strength as compared to most other materials.

2. Reinforced concrete has great resistance to the actions of fire and water and, in fact, is the best structural material available for situations where water is present. During fire of average intensity, members with a satisfactory cover of concrete over the reinforcing bars suffer only surface damage without failure.
3. Reinforced concrete structures are very rigid.
4. It is a low-maintenance material.
5. As compared with other materials, it has a very long service life. Under proper conditions reinforced concrete structures can be used indefinitely without reduction of their load-carrying abilities. This can be explained by the fact that the strength of concrete does not decrease with time but actually increases over a very long period, measured in years, due to the lengthy process of the solidification of the cement paste.
6. It is usually the only economical material available for footings, basement walls, piers, and similar applications.
7. A special feature of concrete is its ability to be cast into an extraordinary variety of shapes from simple slabs, beams, and columns to great arches and shells.
8. In most areas concrete takes advantage of inexpensive local materials (sand, gravel, and water) and requires relatively small amount of cement and reinforcing steel.
9. A lower grade of skilled labor is required for erection as compared to other materials such as structural steel.

To use concrete successfully the designer must be completely familiar with its weak points as well as with its strong ones. Among its disadvantages are the following:

1. Concrete has a very low tensile strength, requiring the use of tensile reinforcement.
2. Forms are required to hold the concrete in place until it hardens sufficiently. In addition, shoring may be necessary to keep the forms in place for roofs, walls, and similar structures until the concrete members gain sufficient strength to support themselves. Formwork is very expensive. Its costs run from one-third to two-third of the total cost of a reinforced concrete structure, with average values of about 50%.
3. The low strength per unit weight of concrete leads to heavy members. This becomes an increasingly important matter for long-span structures where concrete's large dead weight has a great effect on bending moments.
4. Similarly, the low strength per unit volume of concrete means members will be relatively large, an important consideration for tall buildings and long-span structures.
5. The properties of concrete vary widely due to variations in its proportioning and mixing. Furthermore, the placing and curing of concrete is not as carefully controlled as the production of other materials such as structural steel and laminated wood.

Two other characteristics that can cause problems are concrete's shrinkage and creep. These two characteristics can cause cracks in concrete members. The resulting cracks may reduce the shear strength of the members and be detrimental to the appearance of the structure. In addition, the cracks may permit the reinforcing to be exposed to the atmosphere, thereby increasing the possibility of corrosion.

1.2 High Performance Concrete

Many recent innovations in advanced concrete materials technology have made it possible to produce concrete with exceptional performance characteristics. High performance concrete (HPC) is defined as concrete, which meets special performance and uniformity requirements that cannot always be achieved by using only conventional materials and normal mixing, placing, and curing practices. The requirements may involve enhancements of placement and compaction without segregation, long-term mechanical properties, early-age strength, toughness, volume stability, and service life in severe environments. The importance of HPC to the current construction technology is unquestionable. However, before using this new type of concrete, it is necessary to have sufficient background and understanding on the properties of this concrete. This section describes in details about HPC.

1.2.1 Achievement of High Performance Concrete

For a century, concrete has remained a mixture of aggregates, cement, and water. This third ingredient played two essential roles: ensuring hydration of cement and participating actively in the workability of fresh concrete by giving the material satisfactory rheological properties. During the last ten years, numerous scientific investigations have shown the detrimental effects of excess non-hydrated water on the *strength* and *durability* of concrete. Nevertheless, water is essential to obtain effective rheological properties for placing. This requirement therefore points to the need to explore the ways of *reducing the water content* so as to improve the engineering properties of concrete. At the same time, other research scientists have been focusing on

reconstituting a monolithic or solid rock-like material from a *very compact mix*, placing emphasis on mix design.

Two approaches stood out as ways to obtain high performance. They differ in their physical and chemical nature [43]:

1. *Deflocculation of cement grains* : Deflocculation is achieved by using organic products (such as condensates of formaldehyde and sulphonate melamine or of formaldehyde and naphthalene sulphonate). This is the process by which the cement grains in suspension in water can recover their initial grain size (between 5 and 50 μm for the most part). This first approach leads to an appreciable reduction in the quantity of water necessary since quite a lot of this water is no longer trapped in the cement grain flakes (as it would be in traditional concrete where its contribution to workability is then negligible).
2. *Widening the range of grain size* : This extension is achieved by using extremely fine chemically reactive materials (silica fume, fly ash, calcareous fillers even black carbon, etc.), so that they fill the microvoids in grain packing, thus improving the compactness of the material and at the same time improving the rheological properties of the fresh mix. It follows that the quantity of water necessary for placing the concrete can be further reduced.

The first approach can be used alone and leads to interesting gains in engineering properties, workability, and durability. Obviously, the second approach implies simultaneous recourse to the first, since it is naturally useless to complete the grain size range of the granular material towards very fine elements if priority has not been given to reduce flocculation.

As parts of large-scale projects, different experimental programs have confirmed that, where materials available locally are used, respecting these simple principles offers the possibility of obtaining high performance concrete, measured in terms of characteristic compressive strength, with values between 8,700 psi and 11,600 psi (60 and 80 MPa). And these values can be obtained without any real increase in the basic cost of concrete.

Furthermore, a more precise approach, a stricter choice of basic ingredients, acceptance of a more noticeable increase in cost, absolute obligation to use the two approaches already described, can even now make it possible, using industrial production methods, to obtain strength between 13,000 psi and 20,000 psi (90 and 140 MPa), which the designer may consider essential for a project.

Finally, a different type of approach calling upon carefully selected ingredients (cements and aggregates of exceptional quality, inclusion of polymer, etc.), new production processes (compaction, autoclaving, etc.), new structural design (constraint, etc.) can ensure mechanical strengths of several hundred MPa for new applications for projects where the designer can exceed the usual costs [43]. Paragraphs below explain how superplasticizers and cement additives such as silica fume, fly ash or other calcareous fillers improve the performance of concrete.

Superplasticizers

Water is an essential ingredient in concrete ranking alongside cement. In fact, water that is introduced into concrete during mixing has two functions: a physical function, to give the concrete the right rheological properties, and a chemical function, to contribute

to the development of the hydration reaction. Concrete should ideally have only enough water to develop the final and full hydraulic potential of the cement while providing the rheology needed for easy placement.

Unfortunately, available Portland cements preclude attaining concrete with this characteristic. On one hand, cement particle characterized by many unsaturated superficial electrical charges, have a strong tendency to flocculate when in contact with a liquid as polar as water as can be seen in Figure 1.1. On the other hand, the hydration reaction does not wait until the concrete is in the form before starting. Hydration begins as soon as cement touches water due to the fact that certain cement compounds are very reactive and that Portland cement has a lot of very fine particles, some micrometers in diameter, that are of course very reactive. This explains why when only cement and water are used, it is necessary to use more water than necessary to fully hydrate cement particles, given that concrete needs good workability.

In order to alleviate the flocculation tendency and to reduce the amount of mixing water, certain organic molecules, well-known for their dispersing properties, can be used. The first dispersing molecules, more commonly water reducers, were produced from papermill waste and were called lignosulfonates (Figure 1.2). This by-product was not very expensive and required only simple additional processing to be used successively in concrete.

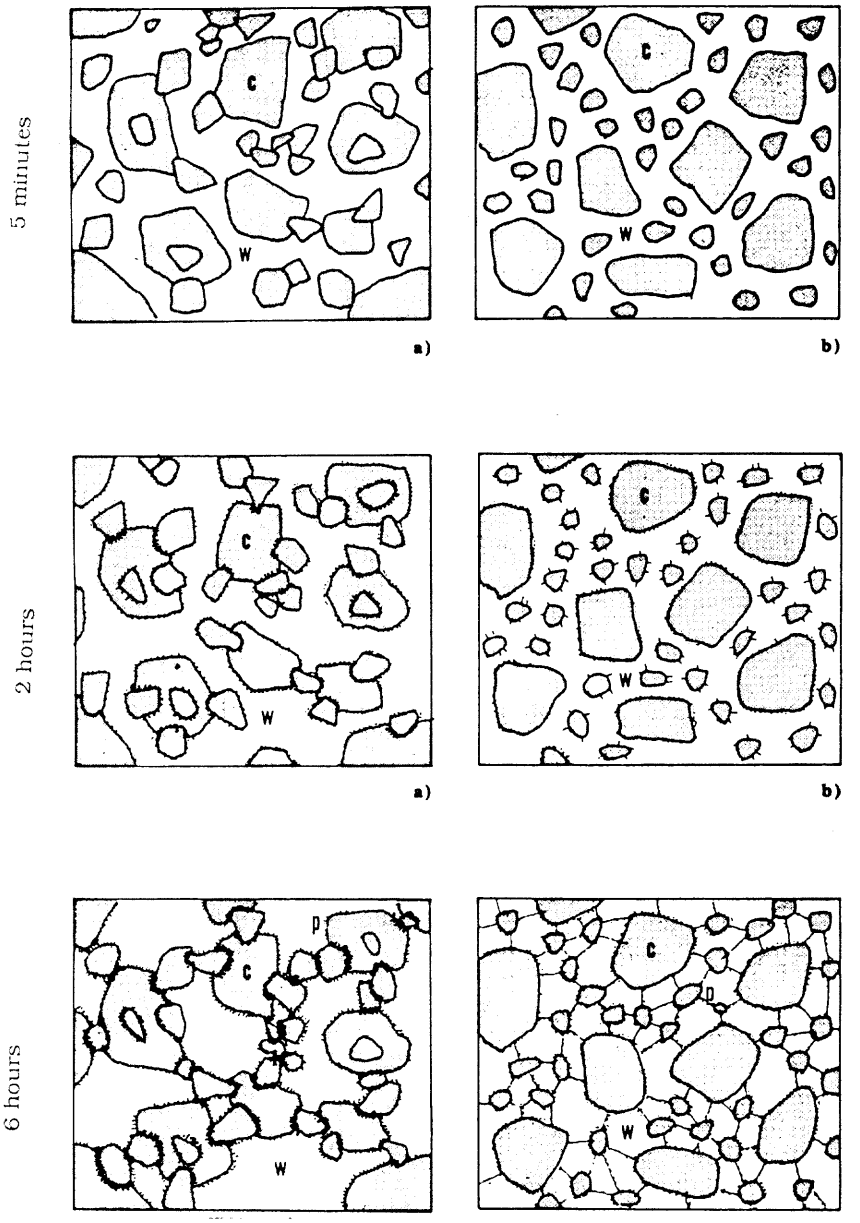

Figure 1.1 Deflocculation of cement grains by a superplasticizer. (Uchikawa, 1986)

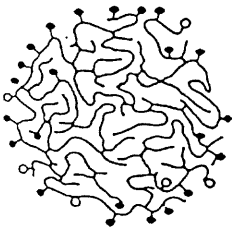

Molecule of
lignosulfonate

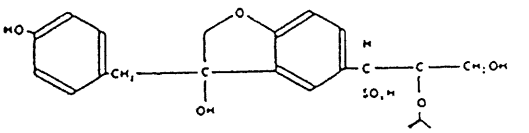

○ COOH Group

● SO_3H Group

R-O-R Linkages

Figure 1.2 Schematic representation of a molecule of lignosulfonate. (Rixom, 1978)

It was rapidly discovered, however, that the dosage could not be increased at will without secondary drawback

- excessive retardation due to the present of sugars in the wood
- entrapment of big air bubbles caused by surfactants.

Other types of molecules were unsuccessfully tried to overcome these drawbacks.

Chemically, water reducers can be anionic, cationic, or even nonionic. They are composed of molecules having a highly charged end that neutralizes one electrical site on a cement particle with an opposite charge. In the case of nonionic water reducer, these molecules act like dipoles that are glued to the cement grains. Figure 1.3 illustrates the mode of action of the three types of water reducer molecule [Aitcin, 1992].

In 1897, Feret gave an expression of the compressive strength as follows :

$$\sigma_c = A \cdot [V_c/(V_c + V_w + V_a)]^2 \qquad (1.1)$$

With V_c, V_w, V_a respectively the volume of cement, water, and air. After applying this formula, reducing the water/cement ratio leads to an increase in strength. However, there is a limit of the water/cement ratio related to the workability of the fresh concrete.

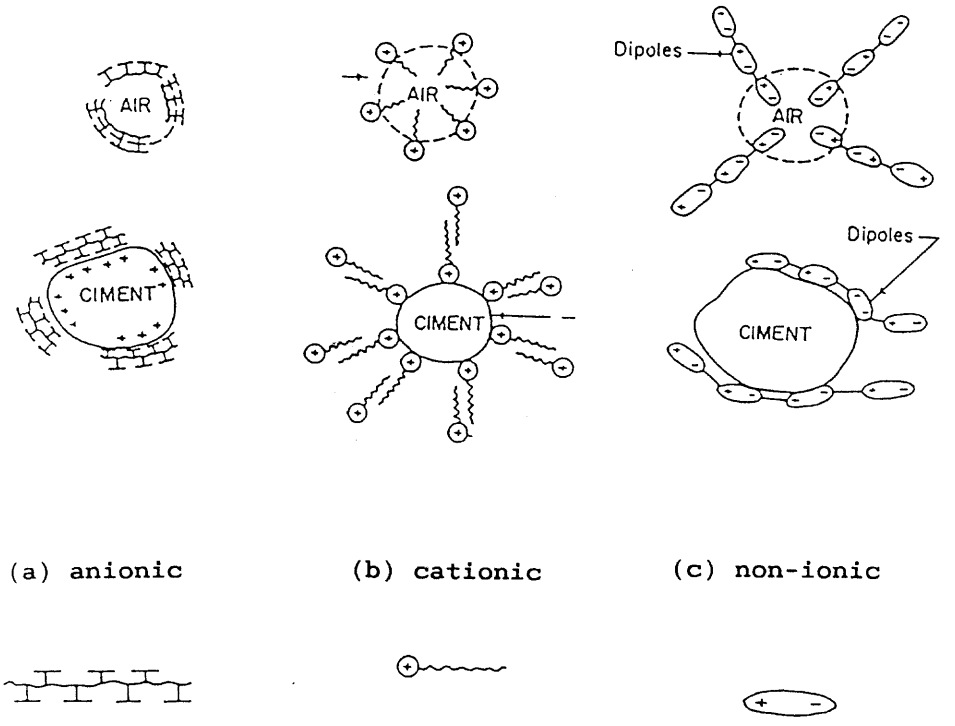

Figure 1.3 Mode of action of water reducers. (Joisel, 1973)

Silica Fume

A normal hardened Portland cement paste is a heterogeneous and porous material. Most of the hydrate appears as an amorphous C-S-H gel, which can take a variety of morphologies like spiny C-S-H. Of the crystalline products ettringite is in the form of rods or fibers with $Ca(OH)_2$ and AF_m phase as hexagonal platelets. These morphologies are seen most clearly on the fracture surface of specimens a few days old and they become less distinct with age. The overall porosity of 25 to 30% in volume comprises two pore families: (1) gel pores related to the silicate C-S-H structure, a few nanometers in size and (2) capillary pores between the various hydrates, formed of air bubbles and microcracks from several hundred nanometers to a few millimeters in size or length.

Compared to materials like steel or sintered alumina, a Portland cement paste develops low mechanical strength during its hardening. The weakness of these

mechanical performances has been mostly related to the capillary porosity and to the excess of water needed for the workability of the fresh paste. Improvement can be achieved by various procedures, one of them is the using of a new material called DSP.

DSP referring to Densified Systems containing homogeneously arranged, ultra-fine Particles is composed of a matrix of Portland cement grains (0.5 to 100 μm size) and ultra-fine particles of silica (5 nm to 0.5 μm) packed in the interstitial space between clinker grains. The microsilica of silica fume, a by-product of the electrometallurgical industry plays a double role: first as a filler and then as a pozzolanic material, which reacts with $Ca(OH)_2$ liberated by C_3S. A superplasticizer is needed for dispersing the silica particles and for avoiding the formation of a gel-like layer which leads to agglomeration. Compressive strengths as high as 270 MPa have been measured on such materials.

The C-S-H form is amorphous and of low porosity (Figure 1.4). The fracture is transgranular. The pozzolanicity of the silica fume can be characterized by its ability to react with $Ca(OH)_2$. In the mixture of OPC + 30% silica all the $Ca(OH)_2$ liberated by the hydration of clinker silicates has been consumed by this microsilica. The Ca/Si ratio of C-S-H is systematically lower in calcium than that of Portland cement and the higher amount of silica fume the lower the C/S (Table 1.1), but inversely, they contain more alkalis respectively 1.3 and 0.5% K_2O for example [29].

Cement	Ca/Si
Portland Cement OPC	1.6
OPC + 13% silica fume	1.3
OPC + 28% silica fume	0.9

Table 1.1 Ca/Si ratio of C-S-H measured by Electron Probe Microanalysis after 200 days hydration. (Regourd, 1981)

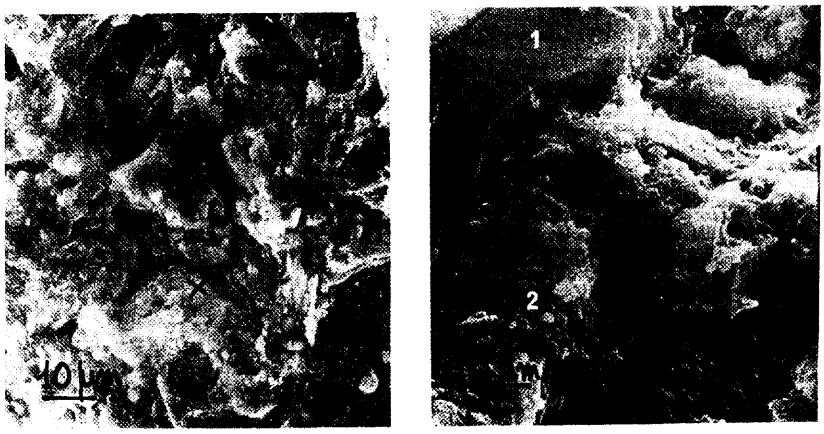

Figure 1.4 Microstructure of a compacted and low water/cement + silica fume paste (28 days). (Diamond, 1976)

Fly Ash

Fly ash, a by-product of coal burning thermal power plants, is generated in large quantity each year. Only a quarter of these by-products was used mostly in the cement and construction industry while the remaining three quarters went to disposal landfills. Shortage of landfills due to environmental concerns has resulted to the escalation of disposal cost of all waste. The Environmental Protection Agency (EPA) estimated in 1987 that the total cost of waste disposal at coal fired plants ranged from $11 to $20/ton for fly ash and bottom ash and potentially will get higher.

Fly ash has a complex characteristic, differing in fineness, morphology, mineralogical composition, and glass content. These characteristics of fly ashes tend to affect the hydration process, the hardening, and the microstructural development of the blended cement paste system. Lane and Best summarized the advantage and disadvantage of fly ash for use in the concrete industry. The advantages are: (1) improve workability, (2) reduce segregration, (3) reduce bleeding, (4) reduce heat evolution, (5) reduce drying shrinkage, (6) increase resistance to sulfates, (7) increase ultimate tensile and

compressive strength, and (8) reduce permeability. The disadvantages when fly ash replace cement on a one-to-one ratio by weight are: (1) lower early strength, (2) lower resistance to freezing and thawing, and (3) increase air-entraining admixture requirement for equal air content [32].

Microscopic examination of fly ashes reveals a wide variety of particle sizes and shapes. Grain size may vary from 0.2 to 200 μm, most particles being larger than 1 μm in size. According to Berry [13], the fraction of fly ash with a particle diameter of about 35 μm was found to be the most appropriate for producing high mechanical strength.

In the available documentation, there is broad agreement as to the effect of fly ash and the importance of the decisive influencing parameters. Opinions still differ, however, as to the physical causes of the observed effects. The following observations based on practical experience with concrete containing fly ash are reported:

- Replacing cement by fly ash reduces the water demand of the concrete.
- The use of fly ash improves concrete pumping or in some cases is a necessary prerequisite for it.
- The workability and, especially, the compactability, flowability, and plasticity of concrete are generally improved.
- The work required to cast and compact concrete is reduced, there is less risk of surface shrink holes.
- Agglomeration capacity is improved and the problem of de-mixing is consequently alleviated.
- Water segregation (bleeding) is reduced.

Reasons reported for the *reduced water demand* of fly ash containing concrete (with reduced percentages of cement) and for the improved properties of freshly mixed concrete are both spherical shape and plain surface (ball bearing effect) and also improve grain size distribution in the range of the finest particles (filling effect) and gravitational forces respectively [41].

The effect of fly ash on the hydration of cement and clinker minerals appears to be complex, and may depend greatly on the chemical and physical nature of the fly ash. Generally, however, there appears to be retardation of the very early hydration of both C_3S and C_3A, as shown by heat evolution profiles over time. After the induction period, however, this is followed by increased formation of $Ca(OH)_2$ and C-S-H and also by increased formation of ettringite and its subsequent transformation to monosulphoaluminates. The prolongation of the induction period in C_3S hydration is probably due to the species dissolved from the fly ash into the aqueous phase of the hydrating system such as aluminate ions and organics which could delay the nucleation and crystallization of $Ca(OH)_2$ and/or C-S-H. There may also be a physical effect in which the fine fly-ash particles adhere to the surface of cement grain and thus hinder its interaction with water.

Once the nucleation and crystallization of hydration products end the induction period, hydration is accelerated by the presence of fly ash. The fly-ash particles provide additional surfaces for the precipitation of the hydration products which would otherwise be formed on the surface of the C_3S, and hinder its interaction with water. Similar arguments may apply to the hydration of C_3A, where the initial retardation is probably due to calcium sulphate and alkalis (in addition to organics) dissolved from the fly ash.

The precipitation of the hydration products on the fly-ash spheres may hinder the pozzolanic reaction. However, the alkaline solution may attack the glassy phase of the spheres beneath the coating of hydration products, leaving a clear space between the coating and the sphere.

A substantial amount of work in the literature suggests that the partial replacement of cement (either by weight or by volume) in mortar or concrete by fly ash results in lower compressive strength at early ages (about 3 to 6 months), with development of greater strength as compared to control concrete at and beyond 6 months (Figure 1.5). The higher later strength is the result of increased pozzolanic reaction at later ages, producing and increasing amount of C-S-H at the expense of $Ca(OH)_2$.

An increased amount of fly ash in the mix delay setting and may slow down strength development at the early ages. High-calcium fly ashes (class D) develop better early strength than low-calcium fly ashes (class F), although they may cause false setting. Faster strength development is achieved by reducing water content and raising curing temperature. Moist or wet curing is found to be beneficial for the strength development of fly-ash concrete.

Partial replacement of cement and fine aggregate by fly ash in the concrete mix results in a concrete with early strength usually comparable to those of control mixes, but with higher strength at later ages. Partial replacement of aggregate, whether fine or both fine and coarse, by fly ash generally produces concrete with increased strength at all ages as compared to control mixes. These observations obviously result from the fact that there is no reduction in cement content in the mix, and that there is increased cement hydration after one day.

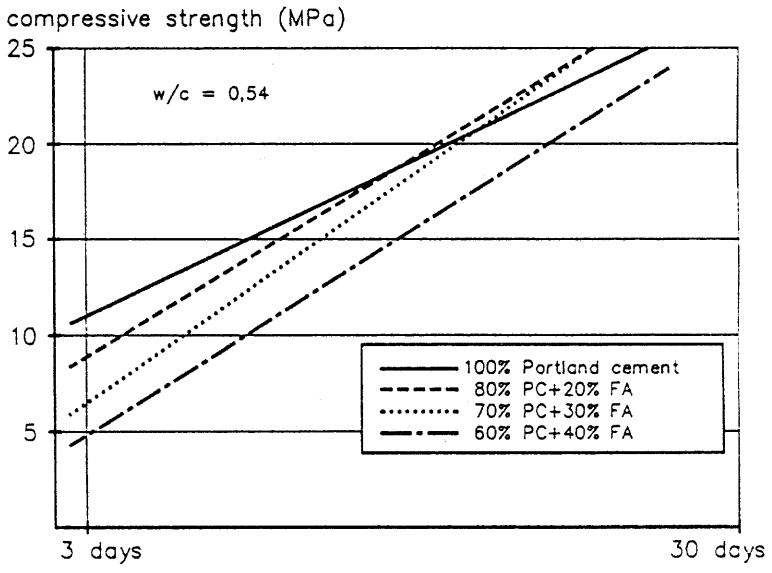

Figure 1.5 Strength development in fly-ash concretes. (Lamond, 1983)

1.2.2 Properties of High Performance Concrete

1.2.2.1 Microstructure. When HPC are formulated, it can be seen that the water content is reduced by spreading out the fine part of their grading. This initial state explains to a large extent the microstructure of the hardened concrete.

According to Regourd et al. [29] & [30], considering the non-solid (liquid or gaseous) volumes of the hardened concrete as gradually refine the scale of observation, it can be found the following "voids":

- Occluded air bubbles, entrained during the mixing of the concrete, in a small quantity because of the fluidity of the HPC (less than 2% of the total volume).
- The paste-aggregate interfaces, favoured positions for the accumulation of water by internal bleeding. But we have seen that there is practically no such bleeding because of the presence of silica fume.
- The void constituted by the vestiges of the intergranular spaces of the fresh paste. These pores are incompletely filled by the hydrates because of "Le Chatelier" contraction (volume loss approximately 10% of the hydration reaction of the-

cement) and failure of a part of the mixing water to combine; this water may be lost by evaporation. But there is a very limited quantity of free water in HPC, because of the low initial water content. Moreover, in this range of w/c ratios, the quantity of hydrates is probably smaller than in an ordinary concrete having the same proportion of cement.

- Finally, on the scale of the nanometer, there are the voids found in the very structure of the hydrates.

Now, observation of a few fragments of hardened HPC with the scanning electron microscope (SEM), we find that the microstructure is very dense, on the whole amorphous, and that it contains an unusual volume of anhydrous grains, cement remains that are uncombined because of a lack of available water. Moreover, the paste-aggregate interfaces are of remarkably low porosity and do not exhibit the usual accumulation of lime crystals. This is due to the pozzolanic activity of the silica fume reacting with the lime released by the cement during its hydration. Mercury porosimetry, a technique rich in information although difficult to interpret because of its partially destructive character, shows a refined structure with practically no capillary porosity. Finally, the ambient humidity in the pores of the concrete can be measured versus the age of the material. Whereas it is always 100% for the usual concretes (in the absence of exchanges with the surrounding atmosphere), it falls to 75% at 28 days for HPC. Finally, these various approaches make it possible to describe the microstructure of HPC as follows:

- A reduced proportion of paste, since the anhydrous grains must be counted as part of the granular skeleton of the hardened concrete.
- A paste of low total porosity.

- Smaller pore sizes (pore grading).
- Very little free water, since only the smallest pores are saturated with water.
- Paste-aggregate interfaces that are no different from the core of the paste, eliminating a traditional zone of weakness of hydraulic concretes.
- A low free lime content.
- A state of self-stresses illustrated macroscopically by the endogenous shrinkage, which undoubtedly leads to a powerful confinement of the aggregates.

1.2.2.2 Main Mechanical Properties. In this section, the main mechanical properties of concrete including compressive strength, tensile strength, Young's modulus (modulus of elasticity), shrinkage, and creep, are mentioned. Good understanding about these properties is important when working with concretes.

Compressive Strength

This is the most important of the material's functional properties. It is also the one that is most spectacularly improved when compared to normal strength concrete. The kinetics of the strength increase are notably faster than that of conventional concretes (see Table 1.2). This results from the initial proximity of the grains of cement in the fresh concrete and from the accelerating action of silica fume mentioned above. How early the strength values appear will depend in practice on the nature (aluminates content, fineness of grinding) and proportion of cement, on the proportion of set retarder, if any, and of course on the temperature of the concrete.

To explain these high strength values, we have given a physical description of the fracture of concrete in compression, which would seem to occur by successive buckling

of the microstructure of the hardened cement paste, then on a larger scale, of the elementary granular edifice called a small column. Using a structure made up of bars to model the matrix of the material, it is easy to show that the compressive strength should increase with the square of the compactness of the hardened cement paste, defined as the proportion of the solid phase by volume, while the tensile strength increases only in proportion to the first power of this value (Feret's law). This is roughly what is found in practice.

Age (days)	1	3	7	14	28	90	360
Mean compressive strength (MPa)	27.2	72.2	85.6	92.6	101.0	109.6	114.1
Splitting strength (MPa)	2.2	5.4	6.4	6.1	6.5	-	-
Modulus of elasticity, E (MPa)	34.9	48.7	51.2	52.4	53.4	53.6	56.8

Table 1.2 Evolution of the mechanical properties of the VHP concrete. (De Larrard & Malier, 1989)

Tensile Strength

This increase is significant, even though the extent of its magnitude is smaller than the compressive strength for the reason stated above. The ratio f_t/f_c therefore decreases to as little as 1/20 in the strongest concretes. However, splitting strength values greater than 870 psi (6 MPa) can be attained, an advantage on which structural engineers can easily turn to account especially in prestressed concrete.

The tensile strength values are attained even faster than the compressive strength values (see Table 1.2). The densification of the matrix and of the paste-aggregate interface explain the improvement of the tensile strength. During splitting tests, the fracture faces are systematically transgranular even with siliceous aggregates, proving the

mechanical homogeneity of the material. It may however be wondered why the tensile strength ceases to increase at approximately 14 days of age, unlike the compressive strength, which may increase by a further 10 to 20%. The state of tension of the matrix, resulting from blocking of its shrinkage by the aggregates, may explain this phenomenon. It may be also a structural effect on specimens preserved in water; the skin of which would tend to swell, causing internal tensile self-stresses that increase as time passes.

Young's modulus

Hashin [19] has proposed mathematical expressions derived from homogenization theories that illustrate the influence of three key parameters; the volume of aggregate (g), the modulus of the paste (E_p), and the modulus of the aggregate (E_a); on the modulus of concrete (E).

$$E = E_p \cdot [(1-g)E_p + (1+g)E_a] / [(1+g)E_p + (1-g)E_a] \qquad (1.2)$$

The modulus of the paste will be governed by its packing density, with an exponent that is logically close to 1. The terms g and E_a do not differ much between a conventional concrete and a HPC. This leads to a rather moderate increase in the modulus, which range from 5.8×10^6 psi (40 GPa) for high-paste HPC with a rather flexible aggregate to approximately 7.9×10^6 psi (55 GPa) for HPC with a skeleton that is densely packed.

The growth of the Young's modulus with time roughly follows that of the tensile strength, without however showing the same tendency to level off from 14 days. Here again, the empirical formula of the regulations relating modulus and characteristic compressive strength, can be extended with out difficulty:

$$E_{ij} = 11{,}000 \cdot (fc_j)^{1/3} \qquad \text{(all quantities in MPa)} \qquad (1.3)$$

Shrinkage

It is drying shrinkage that is of interest here. Figure 1.6 shows the shrinkage of a specimen removed from the mold at 24 hours, having dried in a room in which the relative humidity (50±10%) and temperature (20±1°C) were controlled. The desiccation shrinkage is by convention taken to be equal to the difference between the total shrinkage and the shrinkage of the same specimen with no loss of water. Table 1.3 gives the shrinkages at the end of the experiment and in the long term (extrapolations).

While the final endogenous shrinkage is roughly doubled, the drying shrinkage is greatly reduced, since the material contains very little free water after hydration. The total shrinkage of the HPC, measured on specimens 160 mm in diameter, is approximately half that of the same specimens made of the control concrete. The especially rapid kinetics of the shrinkage of the HPC, which could lead to errors if comparison were made on the basis of short-term tests, should be noted.

	Control concrete	VHP concrete
Total shrinkage	470	320
extrapolation	650	340
Endogenous shrinkage	120	200
extrapolation	120	220
Desiccation shrinkage	350	120
extrapolation	530	120

Table 1.3 Comparative numerical values of shrinkage (in μm/m) measured on the control and VHP concretes. Allowance is made for the initial hydration shrinkages before mold released. (De Larrard & Malier, 1989)

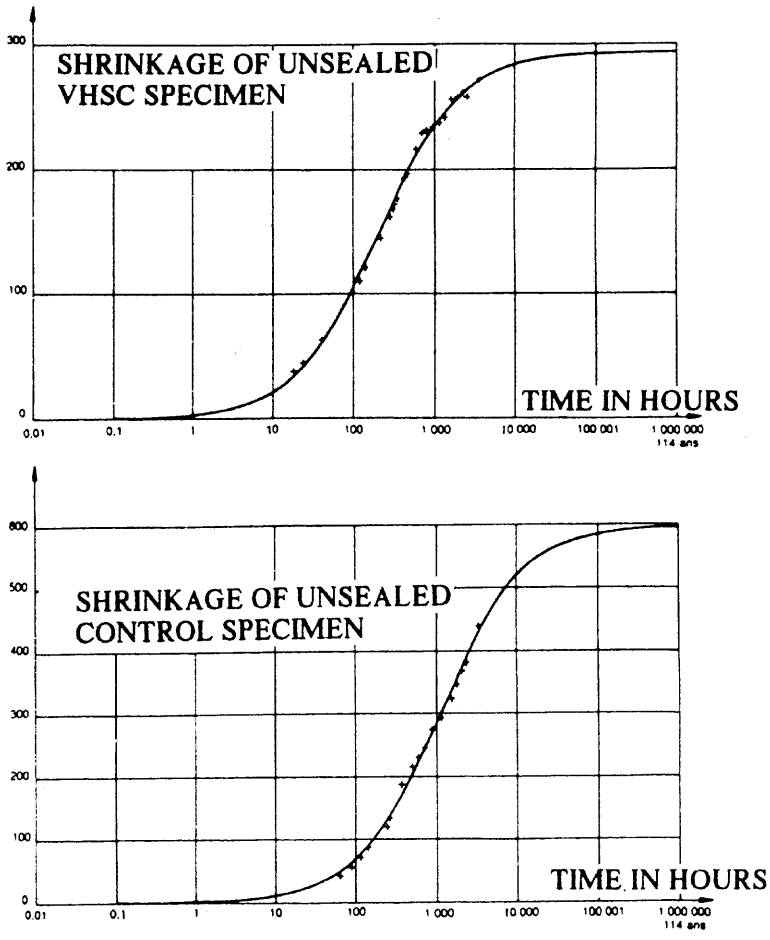

Figure 1.6 Drying shrinkage of VHPC, compared with the one of control concrete (measured on 160x1,000 mm cylinder, reference length 500 mm, at 20°C and 50% R.H.). (De Larrard & Malier, 1989)

Creep

In the experiment of De Larrard [14], The strain versus time can be seen in Figure 1.7 of specimens identical to those used to measure the shrinkage can be seen. The basic creep is in principle determined as the difference between the strain of the loaded specimen coated with resin and that of the equivalent specimen with no load. With the uncoated specimens (preserved under a polyane film for 28 days, then exposed to a

controlled atmosphere, the same calculation gives the *total* creep; the sum of the basic creep and of an additional strain conventionally called desiccation creep.

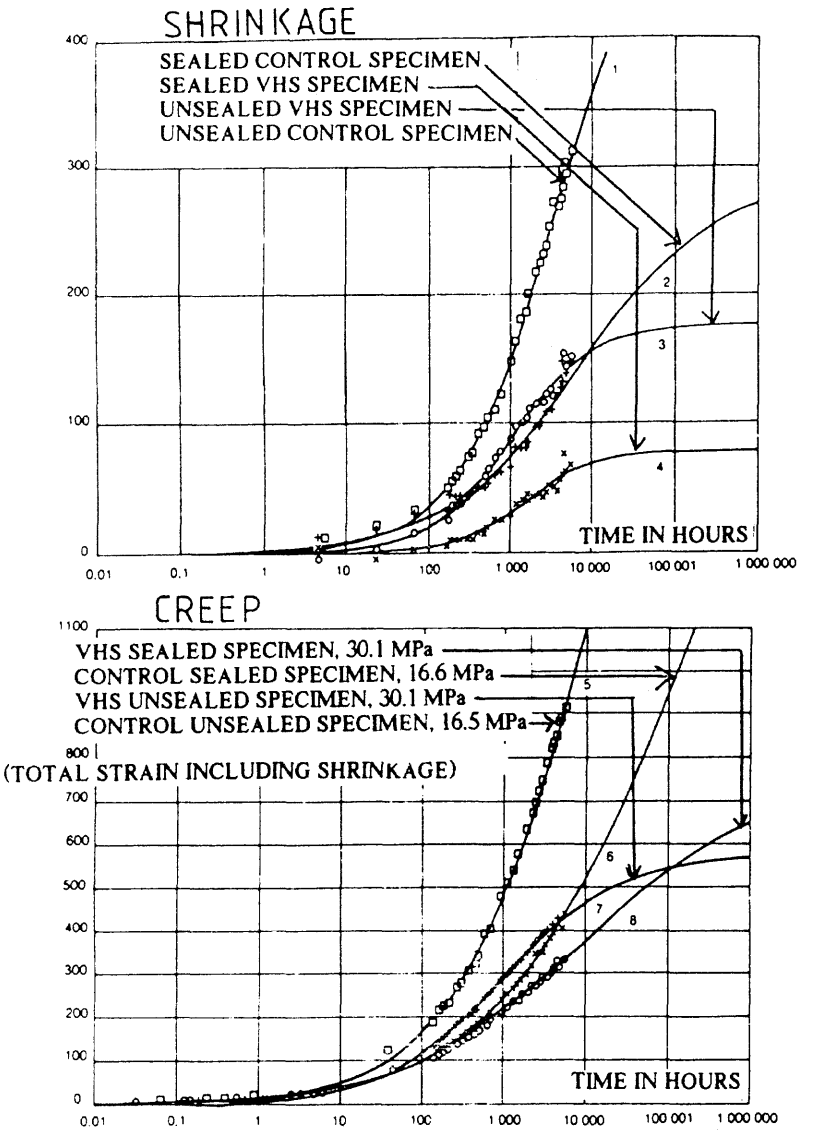

Figure 1.7 Shrinkage and creep of VHPC and control concrete from the age of 28 days. Between the casting and the beginning of measurements, the unsealed specimens have been cured under plastic sheets. After 28 days, the specimens have been air-cured (20°C and 50% R.H.). (De Larrard & Malier, 1989)

In his experiment, the moisture barrier was not as effective as in the shrinkage measurements, because there was no aluminium foil between the two coats of resin. The basic creep of the control is therefore probably slightly overestimated. However, the HPC exhibits the same creep on both specimens. It is therefore unaffected by the foregoing artifact.

The creep of the HPC is finally characterized by:

- rapid kinetics (at 7 days' loading, 67% of the strain at one year is already attained, against only 41% for the control).
- A very low amplitude ($K_{cr} \leq 0.6$, against nearly 2 for the control; this point is perhaps less favorable for loading at a very early age; we found in a previous study K_{cr} near 4 for 1 day old HPC loading).
- Independence of the effects of moisture and of the geometry of the structures, a veritable boon for the structural engineer, who, with these materials, will at last be able to believe in the validity of his calculation.

1.2.3 High Performance Concrete in Recent Constructions

The concrete producers trying to make high performance concrete at the beginning of the 1970s were facing a difficult challenge with the materials available. It was practically impossible to lower the water/cement ratio of the concrete below 0.40 and still provide workability acceptable to the contractor.

With the development of superplasticizers, synthetic water reducers able to disperse cement grains much more efficiently without any secondary effects for dosage ten times

that of lignosulfonate, concretes with water/cement ratios between 0.20 and 0.30 became possible.

The marketing of silica fume, an industrial by-product from the fabrication of silicon metals and ferrosilicon alloys, helped concrete producers to produce low water/cement ratio mixtures. Nowadays, field concretes having water/cement ratios between 0.20 and 0.30 with 200-mm slump one hour after mixing can be delivered. In recent construction works, high performance concretes are widely used in different types of structures because of their advantages to the conventional concretes as mentioned in the previous section. From the current knowledge of HPC, the benefits of HPC in recent construction technologies for each type of structure can be summarized as described below:

Building

- Higher strength in columns and shear walls especially in the lower floors.
- Good workability concretes for concrete pumps in high-rise buildings.
- Increase beam span lengths and then more room available space.

Bridge

- Great regularity of workability and strength properties.
- Substantially improved workability.
- Reduction in superstructure dead loads.
- Increase of span length of precast beams.
- Reduction in number of supporting girders.

Underground Structures

- High resistance to severe aggressive environments.

- High compressive strength.
- High durability.
- Water tight due to low porosity.
- Good workability for complicate parts of structure.

Offshore Structures

- Due to its excellent workability, allows economical fabrication of precast elements of high complex and accurate geometry.
- Allows the reduction of the size of the structures.
- Improve durability of the structures.

Prestressed Concrete

- High compressive strength.
- Low creep and shrinkage.
- Increase durability.

Nuclear Power Plant

- Good resistance to corrosive water.
- Good compactness.
- Good resistance to freeze/thaw cycles.
- Minimum porosity.
- Low shrinkage and low cracking.

1.3 Scope and Objectives of the Research

As mentioned in the previous section, many recent innovations in advanced concrete materials technology have made it possible to produce concrete with exceptional

performance characteristics. High performance concrete (HPC) is defined as concrete that meets special performance and uniformity requirements that cannot be always be achieved routinely by using conventional materials and normal mixing, placing, and curing practices. The importance of HPC to structural engineering is unquestionable. However, HPC is a relatively new material. Some results of researches on conventional concrete are not entirely applicable. The validity of those results for high performance concrete should be investigated.

Even though high performance concrete is very useful for recent construction technology, the major problem of HPC is the insufficient ductility. To investigate the ductility of HPC, the entire stress-strain curve, especially in the descending branch, shall be recorded. More understandings of the ductility of HPC can help structural engineers to evaluate the degree of increasing the ductility of HPC and make the using of HPC safer. Moreover, the total area under the stress-strain curve also represents the amount of energy absorbed by the specimen under loading.

Study about cracking characteristics of HPC is one of the most important investigations of HPC. Many former researches have shown that cracking characteristics of HPC are different from those of normal strength concrete (NSC). The reason is the differences in microstructure properties of these two types of concrete. This experiment focuses on the cracking characteristics of both types of concrete at various stages of strain under uniaxial compression.

The study of stress-strain behavior of concrete under cyclic loading is also included in the experiment to investigate the amount of hysteresis during unloading and reloading cycles, especially in the post-peak stress level of concrete. The magnitude of the

hysteresis is a measure of the amount of energy dissipation due to formation during the loading cycles. Cyclic loading test is also useful for studying the pattern of stiffness degradation in axial direction.

The objectives of this research are:

1. To compare mechanical properties, such as modulus of elasticity and Poisson's ratio, of HPC with those properties of NSC.
2. To achieve the entire stress-strian curve of HPC under uniaxial compression, which can be used to investigate the ductility of HPC.
3. To study cracking characteristics of HPC at various stages of strain under uniaxial compression compared with those of NSC.
4. To study the stress-strain behavior of NSC and HPC under cyclic loading, which is useful to measure the amount of energy dissipation during the loading cycles and study the pattern of stiffness degradation in the axial direction.

CHAPTER 2

LITERATURE REVIEW

2.1 Mechanical Properties of Concrete

Mechanical properties of hardened concrete are the most important property which civil engineers or everyone who work with concretes should pay attention. These properties are compressive strength, modulus of elasticity, Poisson's ratio, tensile strength, creep, and shrinkage. In this research, the first three properties of HPC were investigated. Background knowledge of these properties are described below.

2.1.1 Compressive Strength

Compressive strength of concrete is the most significant property of hardened concrete because any other strengths of concrete such as tensile, flexural, shearing, and bond strength are all related to the compressive strength. For this reason, it means that concrete with high compressive strength will also enhance other properties. Compressive strength of concrete can be found by following ASTM C39. Concrete cylinders are loaded uniaxially by using standard testing machine until the specimens fail. The compressive strength is defined as the maximum compressive load divided by cross-sectional area of the specimen.

There are many factors contributing to the compressive strength of concrete. These are concrete mixtures, water-cement ratio, curing method, shape and size of specimen. Figure 2.1 shows the relationship between compressive stress and compressive strain of concrete in uniaxial test. From the point of zero stress up to 40-50% of the ultimate compressive strength, which is the service range of concrete, the stress-strain relationship

is almost linear since concrete is an inelastic material. However, in practice, when concrete is subjected to service, short-time loading, the stress-strain relationship is usually assumed to be linear.

Beyond the service range, the stress-strain relationship of concrete shows a parabolic behavior. Generally, when concretes reach their maximum compressive strengths, the corresponding strains are usually around 0.002. After the peak strengths, concretes are still able to resist the compressive load while the strains keep increasing. However, concrete stresses continue to decrease until they fail at the strain of about 0.003-0.004 (in/in) depending on their ultimate compressive strengths. Note that, for higher strength concretes, the compressive stresses drop faster than those of lower strength concretes after passing the peak strengths. Accordingly, it can be concluded that lower strength concretes have more ductility than higher strength concretes.

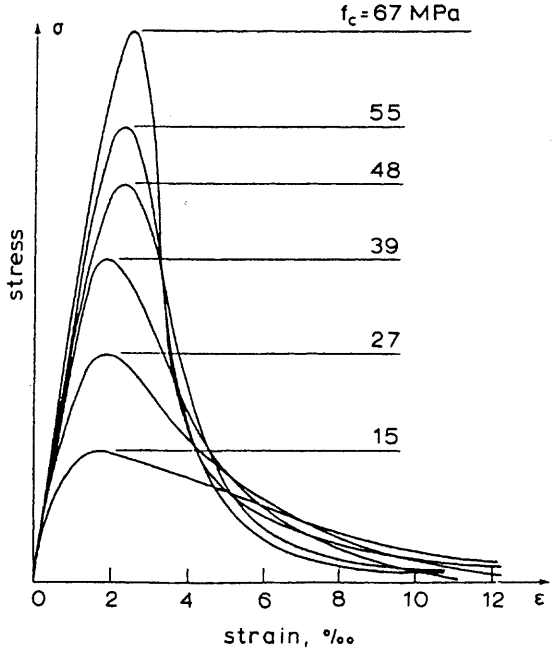

Figure 2.1 Stress-strain curves for cylinders of concrete subjected to uniaxial compression.

2.1.2 Modulus of elasticity

Modulus of elasticity of concrete, E_c, is an indicator of the resistance to deformation of concrete, which is subjected to compressive load. According to many researches in the past, modulus of elasticity of concrete is effected by many factors, such as compressive strength, unit weight as well as degree and duration of loading. When concrete is loaded in the service range under short-term loading, it can be assumed that concrete is an elastic material and has a linear stress-strain relationship. On the other hand, when concrete is subjected to sustained loading or repeated loading, the stress-strain relationship is not linear anymore and engineers have to consider the plastic strain or creep strain because of the gradual decreasing of modulus of elasticity when concrete has more deformations.

There are three different kinds of modulus of elasticity: initial tangent modulus, secant modulus, and tangent modulus. Secant modulus is mostly used in civil engineering. It is obtained by calculating the slope of the line linking the initial point (the origin) and the point considered (usually at about 40 or 50 percent of the maximum compressive stress).

Most published empirical formulas for the static elastic modulus of concrete are related to the compressive strength and the surface-dry unit weight of concrete. The formula in ACI-318 for normal strength concrete is based on the extensive work of Pauw. The ACI-318 formula is quoted as

$$E_c = 0.043\rho^{1.5}\sqrt{f_c'} \qquad \text{(MPa)} \qquad (2.1)$$

where ρ is the surface dry unit weight in kg/m^3 in SI units.

It is well-recognized that Eq. 2.1 is only approximate and accurate to within about ±20 percent for normal strength concretes. This is because the elastic modulus of

concrete is highly dependent on the type of aggregate and the mix proportion[1]. The aggregate usually forms three-quarters of the volume of the concrete, and hence has a considerable importance to strength and many other engineering properties, including stiffness.

For high strength concrete, Eq.2.1 has been reported to overestimate the elastic modulus, and ACI-363 has recommended the following formula taken from the work of Carasquillo et al.

$$E_c = (3320\sqrt{f_c'} + 6900)\left(\frac{\rho}{2320}\right)^{1.5} \quad \text{(MPa)} \qquad (2.2)$$

2.1.3 Poisson's ratio

Poison's ratio is defined as the ratio of lateral strain to strain in the direction of loading. It can be seen in the experiment that when concrete is increasingly loaded in the axial direction, lateral strain is also increased and get much higher when reaching the ultimate compressive strength. Poisson's ratio of normal strength concrete ranges from 0.15-0.25, with an average of 0.17. Concrete with higher strength tends to have a lower Poisson's ratio than that of normal strength concrete, which implies that higher strength concrete has less ductility.

2.2 Stress-Strain Behavior of Concrete under Uniaxial Compression

The compressive stress-strain behavior of concrete is a significant issue in the flexural analysis of reinforced concrete beams and columns. Although the explicit knowledge of the shape of the descending part is generally not accounted in most routine designs, Wang [10] indicated that for an accurate and rational design of the structures subjected

to unusual loading such as earthquakes, it is desirable to know the complete stress-strain curve. The entire stress-strain curve of concrete is also useful for investigating the ductility of concrete. Moreover, the total area under the stress-strain curve can represent the amount of energy absorbed by the specimen under loading. Figure 2.1 shows the stress-strain diagrams for monotonic compression, resulting from tests on cylinders of various concrete strengths. From Figure 2.1 it can be seen that the stress-strain curve consists of three parts:

1. The initial, almost linear part (on which the permissible stresses theory was based), which corresponds to an elastic behavior.
2. The second part defined by strains corresponding to stresses equal to about 70% and up to 100% of the concrete strength, which is characterized by a nonlinear behavior of the material, indicated by a gradual reduction of its tangent modulus. Strictly speaking, some nonlinearity appears at strains as low as $0.3f_c'$, beyond which the microcracks already presented in the unloaded concrete (due to shrinkage, temperature effects and other causes) start to propagate. At stresses between $0.5f_c'$ and $0.7f_c'$ adjacent bond cracks at the interface of mortar and aggregates, caused by the different stiffness of the two materials, start to bridge in the form of mortar cracks, due to stress concentrations at the tips of bond cracks (Aoyama and Noguchi, 1979).
3. The third part, along which strain increases while stress decreases (descending branch). This phenomenon, called strain softening is attributed to the unstable propagation of the aforementioned internal cracks, which tend to become macroscopic.

For decades, many researchers developed empirical and semi-empirical stress-strain relationships to describe the behavior of concrete in compression. Sargin[31] proposed the following relationship to describe the stress-strain behavior of concrete in compression.

$$Y = \frac{AX + BX^2}{1 + CX + DX^2} \quad \text{where } Y = \frac{f}{f_o},\ X = \frac{\varepsilon}{\varepsilon_o} \text{ and } \forall X \geq 0,\ 0 \leq Y \leq 1 \qquad (2.3)$$

Later, Attard and Setunge [27] modified this relationship so that two sets of constant A, B, C, and D were found. One set describes prepeak behavior, while the other describes the postpeak response.

In the ascending curve ($\varepsilon \leq \varepsilon_o$), the proposed boundary conditions are:

(a) at $f = 0$, $df/d\varepsilon = E_{ti}$

(b) at $f = f_o$, $df/d\varepsilon = 0$

(c) at $f = f_o$, $\varepsilon = \varepsilon_o$

(d) at $f = f_{pl}$, $\varepsilon = f/E_c$

in which E_{ti} is the initial tangent modulus at zero stress and E_c is the secant modulus measured at a stress of f_{pl} (usually $0.45f_c'$). The initial tangent modulus can be assumed to vary linearly between $1.17E_c$ and E_c for 20 and 100 MPa (2,900 and 14,500 psi) concretes, respectively. For the ascending curve, the constants are given by

$$A = \frac{E_{ti} \cdot \varepsilon_o}{f_o}, \qquad B = \frac{(A-1)^2}{\alpha\left(1 - \frac{f_{pl}}{f_o}\right)} + \frac{A^2(1-\alpha)}{\alpha^2 \frac{f_{pl}}{f_o}\left(1 - \frac{f_{pl}}{f_o}\right)} - 1 \qquad (2.4)$$

$$C = (A-2), \qquad D = (B+1) \qquad (2.5)$$

where $\alpha = E_{ti}/E_c$. A simpler expression for the constant B can be obtained if α is set to unity.

The residual strength as the strain becomes large can be derived from Eq.2.4, and is given by

$$\lim_{\varepsilon\to\infty} f = f_{resid} = f_o \frac{B}{B+1} \tag{2.6}$$

where the constant B is derived for the descending branch (see Eq.2.7).

To define the descending curve in uniaxial compression, one point is needed on the descending curve. Wang et al. [35] suggested the point of inflection. Under uniaxial compression, the coordinates of the inflection point are denoted by the symbols ε_{ic}, f_{ic}, with the subscript i for inflection and c for uniaxial compression. The boundary conditions for the descending curve ($\varepsilon \geq \varepsilon_o$) are

(a) at $f = f_o$, $df/d\varepsilon = 0$

(b) at $f = f_o$, $\varepsilon = \varepsilon_o$

(c) at $f = f_{ic}$, $\varepsilon = \varepsilon_{ic}$

(d) at $\lim_{\varepsilon\to\infty} f_{resid} = 0$

The resulting expressions for the four constants for the descending curve are, therefore

$$A = \frac{f_{ic}}{\varepsilon_c \cdot \varepsilon_{ic}} \frac{(\varepsilon_{ic} - \varepsilon_c)^2}{f'_c - f_{ic}}, \quad B = 0 \tag{2.7}$$

$$C = A\text{-}2 \quad , \quad D = 1 \tag{2.8}$$

Consequently, to establish the full uniaxial stress-strain relationship, the parameters required are uniaxial compressive strength, strain at the peak stress, elastic modulus, and stress and strain at the inflection point.

Based on the analytical expressions of Mander et al.[21] and the experimental results of Dahl[23], the following approximate expressions for the uniaxial inflection point are proposed.

$$\frac{\varepsilon_{ic}}{\varepsilon_c} = 2.5 - 0.3\ln(f_c') \qquad f_c' \text{ in MPa} \tag{2.9}$$

$$\frac{f_{ic}}{f_c} = 1.41 - 0.17\ln(f_c') \qquad f_c' \text{ in MPa} \tag{2.10}$$

Several investigators have proposed linear expressions that are a function of f_c' to predict the strain at peak stress. Popovics[37] suggested that the strain at the peak stress reflects the amount of microcracking that occurs up to the peak stress. A measure of linearity of the ascending branch of the stress-strain curve is the ratio of the elastic modulus to the secant modulus at the peak stress. For normal strength concretes, this ratio is close to 2, and the strain at peak stress is assumed to be 0.002. High strength concretes have a larger range of linearity in the ascending branch, and the strain at the peak stress is also larger than for NSC. The ratio of the elastic modulus to the secant modulus at the peak stress for high strength concrete would therefore be closer to unity. The extent of the linearity of the ascending branch is highly dependent on the aggregate used, and hence any expression for ε_c should be a function of the elastic modulus of the concrete. Setunge[38] proposed the following expression for strain at peak stress of concrete with crushed aggregates

$$\varepsilon_c = \frac{f_c' 4.26}{E_c \sqrt[4]{f_c'}} \qquad \text{MPa} \tag{2.11}$$

Another relationship is the equation originally proposed by Popovics[37], and later modified by other researchers and summarized by Collins et al.[28]

$$\frac{f_c}{f_c'} = \frac{\varepsilon_o}{\varepsilon_o'} \cdot \frac{n}{n-1+(\varepsilon_o/\varepsilon_o')^{nk}} \tag{2.12}$$

$$k = 0.67 + \frac{f_c'}{9000} \tag{2.13}$$

$$n = 0.8 + \frac{f_c'}{2500} \tag{2.14}$$

$$\varepsilon_o' = \frac{f_c'}{E_c} \cdot \frac{n}{n-1} \tag{2.15}$$

$$E_c = 40{,}000\sqrt{f_c'} + 1{,}000{,}000 \tag{2.16}$$

where n and k are curve fitting factor, as n becomes higher, the rising curve becomes more linear, f_c is the compressive stress, ε_o is the compressive strain, f_c' is the peak stress of concrete, and ε_o' is the strain corresponding to the peak stress.

The stress-strain relationships presented by Sargin and Collins imply that the entire stress-strain curve is a material property. While this is a reasonable assumption for the prepeak regime, the postpeak portion of the curve is more complicated. There are many factors which affect the postpeak behavior of concrete in compression. Some significant factors include frictional end restraints between platen and specimens, permissible rotation by the platens, loading rate, and machine stiffness. Another significant factor is the aspect ratio or height-width ratio H/W. Differences in postpeak ductility of specimens with varying aspect ratios have been observed experimentally. Researchers have found significant increases in postpeak ductility as the aspect ratio decreases.

There are rather limited literature about the complete stress-strain curve of high strength concrete. One of the reasons why there are insufficient experimental results on the entire stress-strain curve of high strength concrete is that it is quite difficult to obtain the descending portion of the curve. Nevertheless, it is generally recognized that for high strength concrete, the slope of the ascending part of the curve is more linear and steeper,

the strain at maximum stress is slightly higher, and the slope of the descending part is steeper as compared to normal strength concrete. Carrasquillo et al.[39] suggested that internal difference among normal and high strength concrete in terms of microcracking and failure mode are directly related to the differences in the compressive stress-strain behavior of different strength concrete. To obtain the descending part of the stress-strain curve, it is generally necessary to avoid the specimen-testing machine interaction. The closed-loop testing machine is usually used, so the specimens can be loaded so as to maintain a constant rate of strain increase and avoid unstable failure. For high strength concrete, it may be necessary to use the lateral strains as a feedback signal rather than the axial strains.

2.3 Cracking Characteristics of Concrete Cylinder under Uniaxial Compression

For a heterogeneous material like concrete, cracking is a dominant factor for its behavior, and the development of microcracking is closely related to the characteristics of stress-strain relation. The descending branch is attributed to the extension of continuous cracks, which may be regarded as the reduction of effective cross-sectional area [Meyer and Okamura, 1986]. The descending branch of the stress-strain curve of concrete can no longer be treated as a material property. Rather, it has to be referred as a structural property [40].

The mode of failure of high strength concrete cylinders in uniaxial compression is different from that of normal strength concrete cylinders. The number and length of continuous crack patterns developed at failure decreases as the concrete compressive strength increases. Moreover, it has been observed that the cracking in HSC is more

localized and that it approaches the behavior of a homogeneous material when compared with cracking in NSC. It is also observed that in NSC cracks generally develop between the interface of aggregates and the cement paste. This leads to a distinct interlocking of the crack faces, resulting in increased resistance to failure. On the other hand, in HSC, cracks propagate through the aggregates and, consequently, there is less resistance across crack surfaces due to reduced interlocking. HSC exhibits a very linear load-deformation response prior to peak load and a very brittle behavior after the peak [33].

2.4 Stress-Strain Behavior of Concrete under Cyclic Loading

The earthquake-resistant properties of a material can be evaluated using their stress-strain diagrams, where both strength and deformation characteristics are reflected. The determination of stress-strain diagrams (δ_c-ε_c) for concrete under seismic loading is commonly obtained using experimental set-ups, whereby the material is subjected to repeated loading and unloading without change of sign, or to cyclic loading (involving load reversals); as a rule both tests are of the static type, that is they are carried out at very low loading rates. Correlating the results from such tests with the actual behavior under seismic loading, which is characterized by deformations induced at a very high loading rate is always a safe procedure as far as strength of the material is concerned [17].

Nevertheless, in most cases, accurate quantitative predictions on the load-deformation history up to and beyond the ultimate load remain difficult to obtain. The highly nonlinear nature of concrete stress-strain relationship under a cyclic loading can not be easily described by any mathematical formulas. Figure 2.2 shows stress-strain

diagrams of concrete cylinders subjected to repeated uniaxial compression with full unloading [Karsan and Jirsa, 1969]. It can be observed from the stress-strain curve that the reloading path of the cyclic responses always join the monotonic stress envelop, almost at the level of previously attained maximum stress. The similarity of monotonic and cyclic stress-strain envelops indicates that the specimens subjected to unloading and reloading cycles experience very little or no strength degradation due to cycling, which suggests that the strength criteria for concrete are basically path-independent.

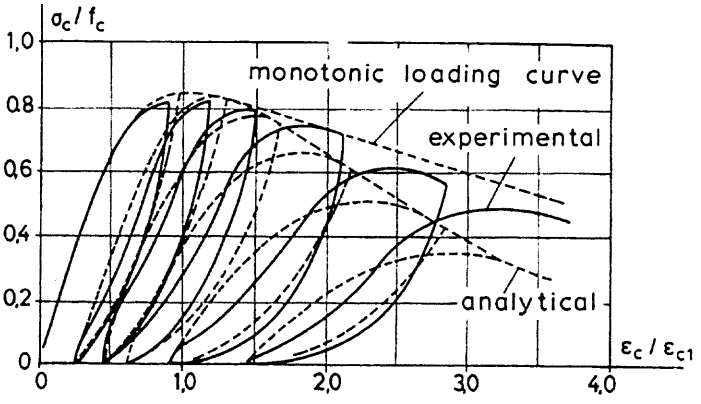

Figure 2.2 Stress-strain diagrams for concrete cylinders subjected to repeated uniaxial compression with full unloading. (Karsan and Jirsa, 1969)

However, the cyclic stress-strain curves exhibit hysteresis during unloading and reloading cycles, especially past the peak stress level of concrete. The magnitude of this hysteresis is a measure of the amount of energy dissipation due to crack formation during the loading cycles. Furthermore, the unloading and reloading curves do not coincide and are not parallel to the initial loading curve. The average slope of the unloading and

reloading curves is inversely proportional to the plastic strain. This implies that there is a definite stiffness degradation for the entire strain range of stress-strain curve.

Ductility; the ability to undergo plastic deformation; constitutes one of the fundamental requirements regarding the mechanical behavior of structural elements in an earthquake-resistant structure. The ductility of an element should be conceived at the same time as: (a) ability to sustain large inelastic deformations without substantial reduction in strength, and (b) ability to absorb and dissipate seismic energy through relative stable hysteresis loops. The ductility factor is defined as the ratio of the ultimate deformation at failure to the yield deformation, δ_u/δ_y. The ultimate deformation at failure is defined for design purposes as the deformation for which the material or the structural element loses only a small, predefined percentage of its ultimate strength (e.g. 15% for concrete). The larger the available ductility factor of a structural element with constant strength, the larger is the safety margins of the element against an earthquake.

CHAPTER 3

MATERIALS AND EXPERIMENTAL INVESTIGATION

3.1 Specimens, Materials and Mixture Proportions

3.1.1 Specimens

In this research, normal strength concrete and high performance concrete were studied. The desired compressive strength (f_c') for normal strength concrete is 5,000 psi (34.5 MPa) at 28 days, and for high performance concrete is 12,000 psi (83 MPa) at 28 days. Test specimens must be straight circular cylinders with ∅ 4x8 in. (10x20 cm.) long in size and within the tolerances specified and prepared in accordance with ASTM C192.

3.1.2 Materials

As described in chapter 1, the strength of concrete mainly depends on the strength of the hydration structure and the porosity of the concrete matrix. Porosity increases with increasing water/cement ratio. Therefore, reducing the water/cement ratio is a method of attaining higher strength concrete, and adding other chemical products is another method of improving the workability of concrete.

The materials used consisted of Type I cement according to ASTM C150, tap water which is clean enough for making concrete, sand from a local source, and limestone with the maximum size of 3/8 in. For high strength concrete, silica fume and Class F-fly ash in powder form were used to achieve higher strength, and superplasticizer was also used to maintain the consistency of the concrete mixes.

3.1.3 Mixture Proportions

Two different mixture categories were prepared to achieve the nominal compressive strengths as mentioned above for NSC and HPC. The mixture constituents for the two mixture categories are given in the Table 3.1 below

Concrete designation	NSC		HPC	
Design strength	5 ksi	34 MPa	12 ksi	83 MPa
Cement	714 lb	424 kg	738 lb	438 kg
Fly ash	-		67 lb	40 kg
Silica fume	-		103 lb	61 kg
Water	356 lb	211 kg	239 lb	142 kg
Coarse aggregate	1843 lb	1094 kg	1666 lb	989 lg
Fine aggregate	1173 lb	696 kg	1308 lb	776 kg
Superplasticizer	-		11.12 litre	
Total weight	4086 lb	2425 kg	4121 lb	2446 kg
w/c ratio	0.5		0.32	
w/cm ratio	0.3		0.26	

Table 3.1 Specimen mixture proportions per yd^3 (m^3)

3.2 Experimental Investigation

All of the mixture constituents above were mixed in a concrete mixer. After demolding the specimens after 1 day of placing, the concrete specimens must be moist cured at 73±3°F (23±2°C) in accordance with ASTM C192. The specimens were air-dried for at least 1 week before testing to reduce the influence of pore pressure on the test results. To find modulus of elasticity and Poisson's ratio of concrete specimens in accordance with ASTM C469, each specimen is loaded at least twice. Data of the first loading is not used. Base calculations on the average of the results of the subsequent loadings. The applied

load, longitudinal strain, and transverse strain, were recorded without interruption of loading at two different points. Which are

1. when the longitudinal (axial) strain is 50 millionths (0.000050)
2. when the applied load is equal to 40% of the ultimate load.

Modulus of elasticity was calculated to the nearest 50,000 psi (344.74 MPa), as follows

$$E = (S_2 - S_1) / (\epsilon_2 - 0.000050) \quad (3.1)$$

where

S_2 = stress corresponding to 40% of ultimate load

S_1 = stress corresponding to a longitudinal strain, $\epsilon_1 = 0.000050$

ϵ_2 = longitudinal strain produced by stress S_2

Also, Poisson's ratio was calculated to the nearest 0.01, as follows

$$\nu = (\epsilon_{t2} - \epsilon_{t1}) / (\epsilon_2 - 0.000050) \quad (3.2)$$

where

ϵ_{t2} = transverse strain at midheight of the specimen produced by stress S_2

ϵ_{t1} = transverse strain at midheight of the specimen produced by stress S_1

To obtain the entire stress-strain curve of concrete under uniaxial compression, especially in the descending part, it is generally necessary to avoid the specimen-testing machine interaction. In this experiment, the MTS-815 closed-loop testing machine is used as shown in Figure 3.1 and 3.2. In a closed-loop testing machine, specimens can be loaded so as to maintain a constant rate of strain increase and thus avoiding unstable failure. The slow rates were used, 1.5×10^{-6} to 3×10^{-6} strain/sec for NSC and $1\text{-}5 \times 10^{-7}$ strain/sec for HPC. For high performance concrete, it might be necessary to use the

lateral strains as a feedback signal rather than the axial strains. A circumferential extensometer attached to the ends of a linked chain with a roller at each hinge is placed around the cylinders at midheight, measuring the circumferential expansion. The circumferential displacement nominalized by the initial cylinder circumference was reported as circumferential strain, which is theoretically equal to the lateral strain. The axial strain was measured on the surface of the cylinder with two compressometers of 4-in. gage length.

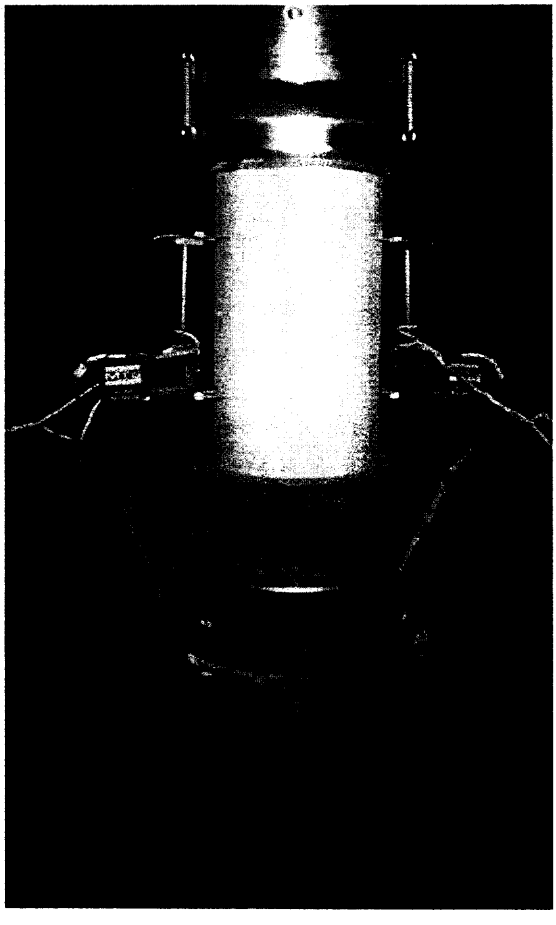

Figure 3.1 Experimental setup for uniaxial compression test.

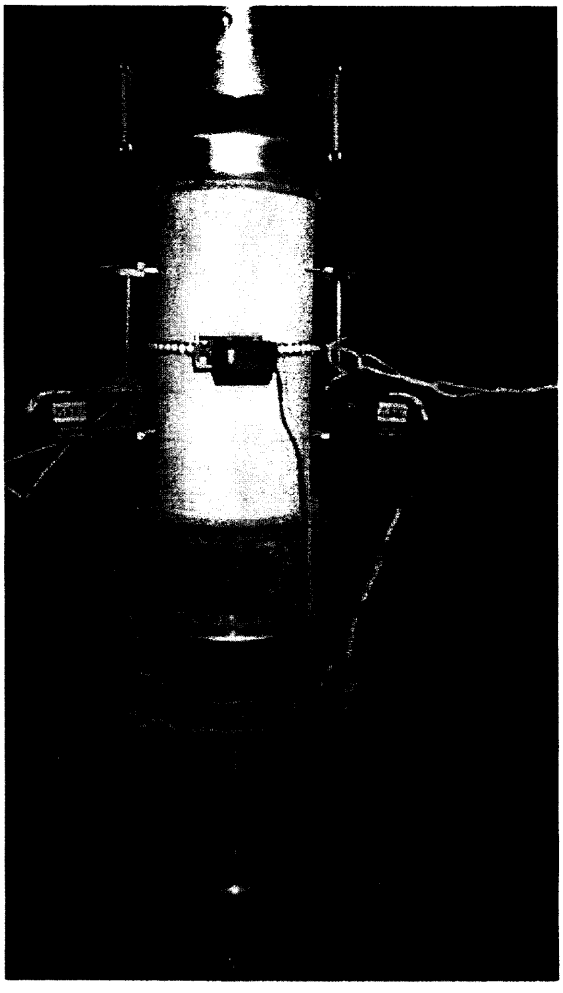

Figure 3.2 Experimental setup for uniaxial compression test with circumferential extensometer.

Cracking characteristics of both types of concrete (NSC and HPC) were investigated by taking the pictures of crack propagation at various stages of strain under uniaxial compression in the post-peak regime. These observations could be achieved by interruption of loading at specified stages of strain, and then continued loading the specimens until failures occurred. The failure patterns were also recorded for comparison of the failure modes of the two types of concrete.

The stress-strain curves obtained for 4 by 8 in. (10 by 20 cm.) concrete cylinders under cyclic loading were also investigated. Pattern of loading is that the unloading starts from the envelop to near zero stress level and then reloading starts from near zero stress level to the envelop curve. These stress-strain curves from cyclic loading were compared to those of the monotonic loading corresponding to each type of concrete.

CHAPTER 4

RESULTS AND DISCUSSION

Plain high performance concrete ($f_c' \geq 10{,}000$ psi or 68.95 MPa) and normal strength concrete ($f_c' \leq 6{,}000$ psi or 41.37 MPa) in cylinders with ∅ 4x8 in. long in size were tested under short-term uniaxial compression at the age of 28 days. Mechanical properties such as compressive strength, modulus of elasticity, and Poisson's ratio were studied for both types of concrete. The entire stress-strain curve, cracking characteristics, and behavior of concrete cylinders of both types of concrete under cyclic loading were also investigated. The results obtained for each type of concrete were compared to each other and also compared with the results obtained by other researchers.

4.1 Mechanical Properties of Concrete

The compressive strength, modulus of elasticity, and Poisson's ratio were obtained in the short-term uniaxial compression tests. The compressive strengths could be found immediately during the tests whereas the modulus of elasticity and Poisson's ratio were calculated per steps as mentioned in Chapter 3. These average results from each batch of both types of concrete are given in Table 4.1. The average results for normal and high performance concrete are shown in Table 4.2. It can be seen from the table that strain at peak stress of normal concrete is usually less than that of high performance concrete. The reason is that the compressive strength ratio between high performance concrete and normal strength concrete is greater than the ratio of modulus of elasticity between the two concretes. The modulus of elasticity of high performance concrete is higher than that of normal strength, as expected. The results show that the equations for determining the

modulus of elasticity provided by ACI 318-99 and ACI 363-88 are applicable for the test results of normal strength concrete, while the equation from ACI 318-99 tends to overestimate the modulus of high performance concrete. The equation from the work of Carasquillo in ACI 363-88 was found to be reliable for predicting the modulus of elasticity of high performance concrete in this experiment. Finally, Poisson's ratio of high performance concrete is less than that of normal strength concrete. However, the difference of Poisson's ratio is not remarkable between the two concretes. It can be concluded that high performance concrete has less lateral deformation when it is subjected to the same magnitude of axial loading than that of normal strength concrete, which means high performance concrete has less ductility than that of normal strength concrete.

Mix	f_c'		ε_o	E_c		Poisson's	E_c^*		E_c'	
no.	(psi)	(MPa)	(in/in)	(ksi)	(MPa)	ratio, ν	(ksi)	(MPa)	(ksi)	(MPa)
NSC-1	5104	35.2	0.00174	4485	30924	0.21	4389	30465	4122	28423
NSC-2	5618	38.7	0.00174	4179	28817	0.20	4605	31944	4270	29445
HPC-1	10077	69.5	0.00235	5030	34683	0.18	6246	43365	5429	37432
HPC-2	10403	71.7	0.00229	5020	34614	0.19	6347	44046	5497	37903
HPC-3	10987	75.8	0.00240	5394	37188	0.18	6522	45288	5622	38761

Table 4.1 The results of mechanical properties of each concrete mix.

where $E_c^* = 0.043\rho^{1.5}\sqrt{f_c'}$ (MPa) or $33\rho^{1.5}\sqrt{f_c'}$ (psi) (ACI 318-99)

$$E_c' = (3320\sqrt{f_c'} + 6900)\left(\frac{\rho}{2320}\right)^{1.5} \text{ (MPa)} \qquad \text{(ACI 363-88)}$$

According to Table 3.1, ρ = 151.33 lb/ft^3 or 2425 kg/m^3 for NSC and
ρ = 152.63 lb/ft^3 or 2446 kg/m^3 for HPC

f_c' = compressive strength concrete
ε_o = strain at peak stress of concrete
E_c = modulus of elasticity
ν = Poisson's ratio

Mix no.	f_c'		ε_o	E_c		Poisson's Ratio, ν
	(psi)	(MPa)	(in/in)	(ksi)	(MPa)	
NSC	5361	36.95	0.00174	4332	29870	0.205
HPC	10489	72.33	0.00234	5148	35495	0.183

Table 4.2 Average results of normal and high performance concrete

4.2 Stress-Strain Behavior of Concrete under Uniaxial Compression

The complete stress-strain curve of both types of concrete under uniaxial compression were obtained by using the MTS-815 closed-loop testing machine. As a result, the specimens could be loaded so as to maintain a constant rate of strain increase and avoid unstable failure. Figure 4.1 to 4.6 show the complete stress-strain curves of concrete obtained from the experiment.

It can be seen from the figures that for high strength concrete, the shape of the ascending part of the stress-strain curve is more linear and steeper, that results in the increase of elastic modulus. The strain at peak stress is slightly higher, and the slope of the descending part is steeper as compared to normal strength concrete. That was due to the decrease in the extent of internal microcracking in higher strength concrete [39].

Ductility of both types of concrete was also studied in this research. The degree of ductility was measured by using the ductility factor (δ_u/δ_y) as mentioned in chapter 2. The results were shown in Table 4.3. It can be seen from the table that normal strength concrete has higher ductility ratio than that of high performance concrete. According to this result, it can be concluded that normal strength concrete has more ability to sustain large inelastic deformation without substantial reduction in strength and the ability to absorb and dissipate seismic energy through relatively stable hysteresis loops.

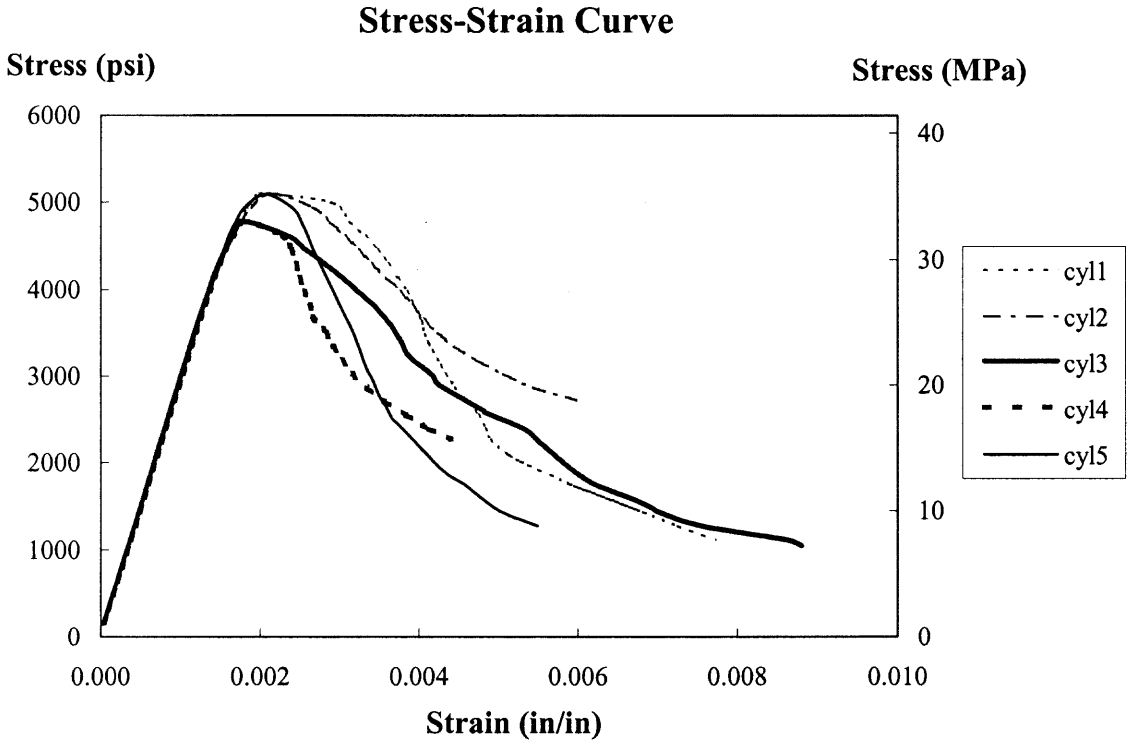

Figure 4.1 Stress-Strain curve of normal strength concrete (NSC-1)

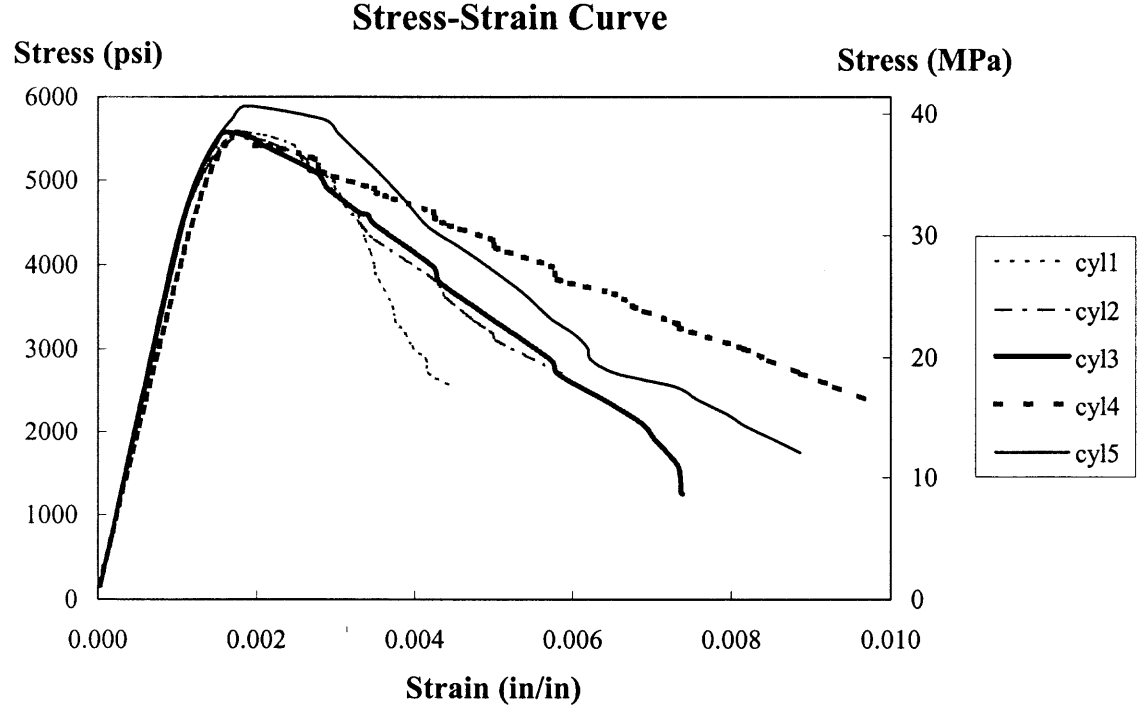

Figure 4.2 Stress-Strain curve of normal strength concrete (NSC-2)

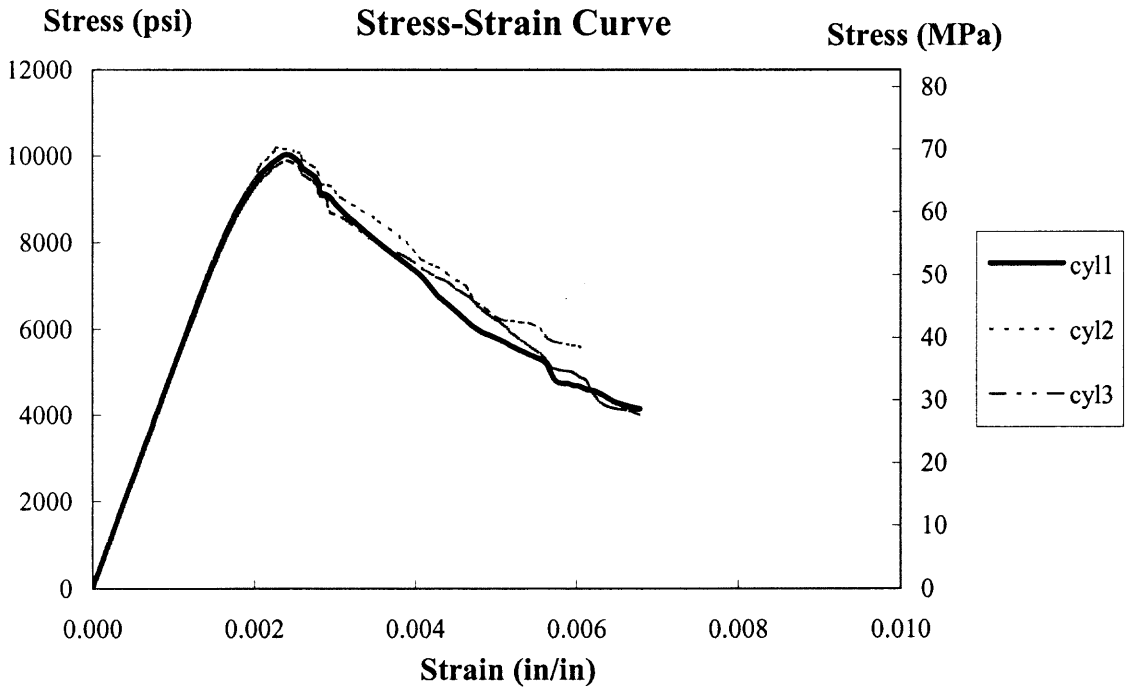

Figure 4.3 Stress-Strain curve of high performance concrete (HPC-1)

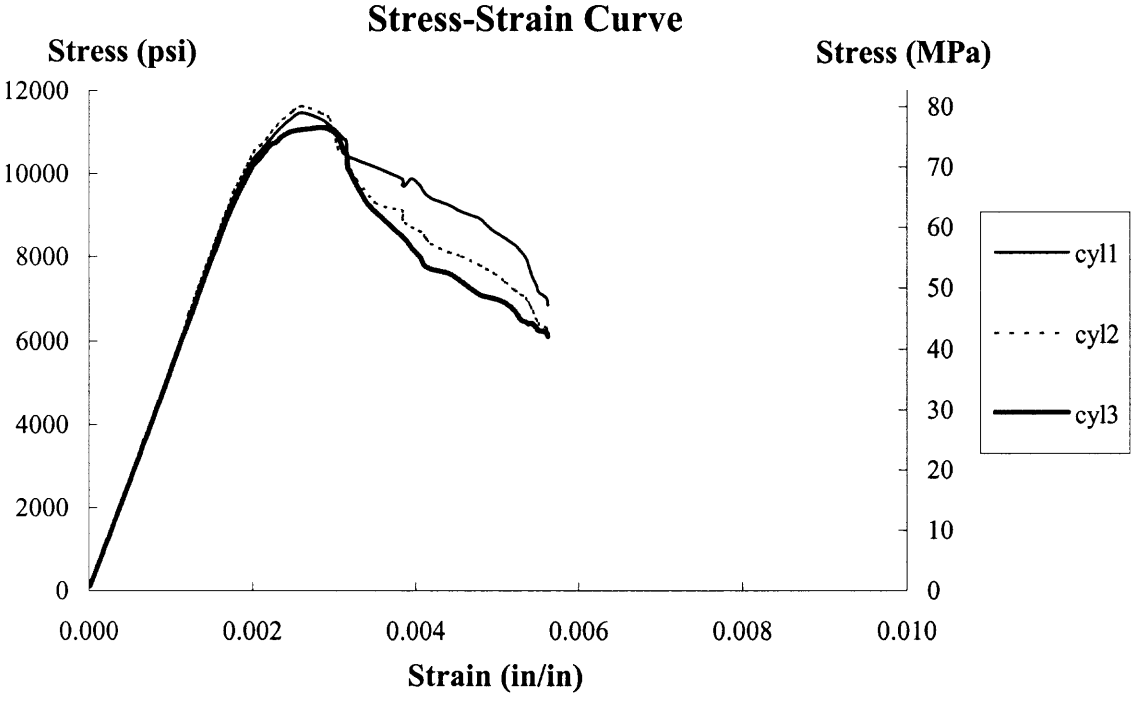

Figure 4.4 Stress-Strain curve of high performance concrete (HPC-2)

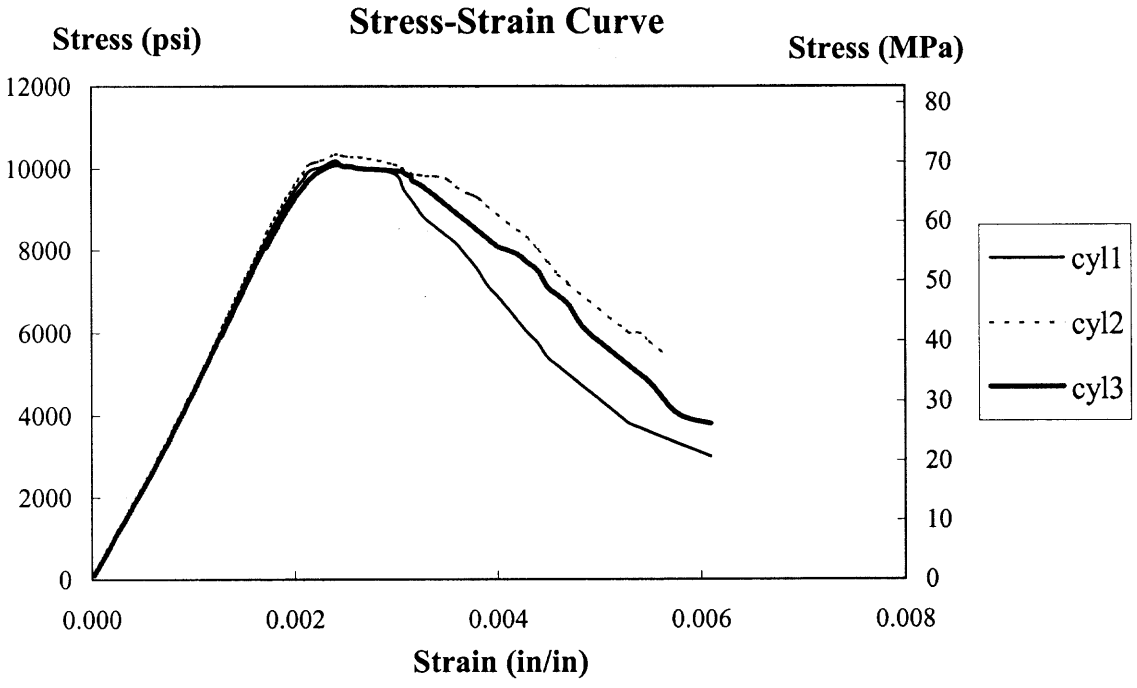

Figure 4.5 Stress-Strain curve of high performance concrete (HPC-3)

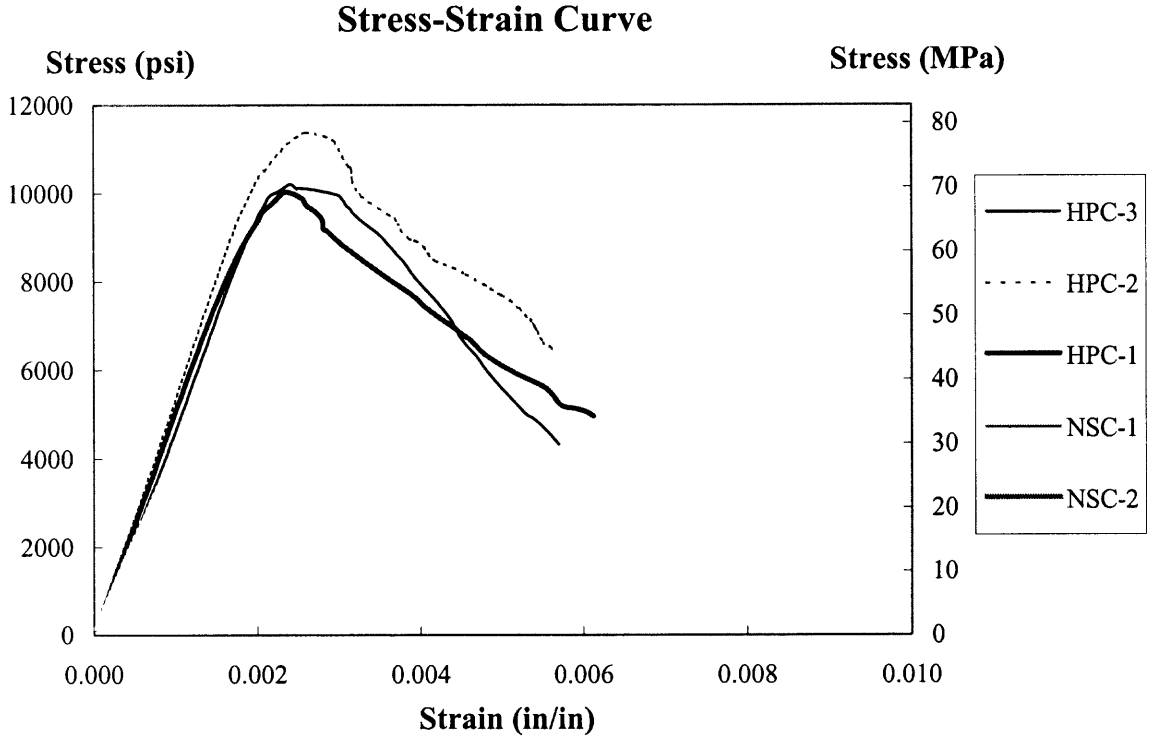

Figure 4.6 Stress-Strain curve of normal strength concrete and high performance concrete.

However, ductility of high performance concrete can be increased by using steel reinforcements, mostly used in the form of lateral confinements such as in columns.

Mix no.	δ_u*	δ_y	δ_u/δ_y
NSC-1	0.02522	0.01790	1.408
NSC-2	0.02709	0.01357	1.997
HPC-1	0.02612	0.01889	1.382
HPC-2	0.02793	0.02085	1.339
HPC-3	0.02947	0.01923	1.532

* δ_u = ultimate deformation at failure, the deformation for which the concrete specimen loses only 15% of its ultimate strength

Table 4.3 Ductility ratio of normal and high performance concrete

Experimental data of normal strength concrete and high performance concrete were also compared with the empirical equations proposed by Sargin (adapted by Attard and Setunge) and Collins as mentioned in chapter 2. The comparison curves are shown in Figure 4.7-4.11.

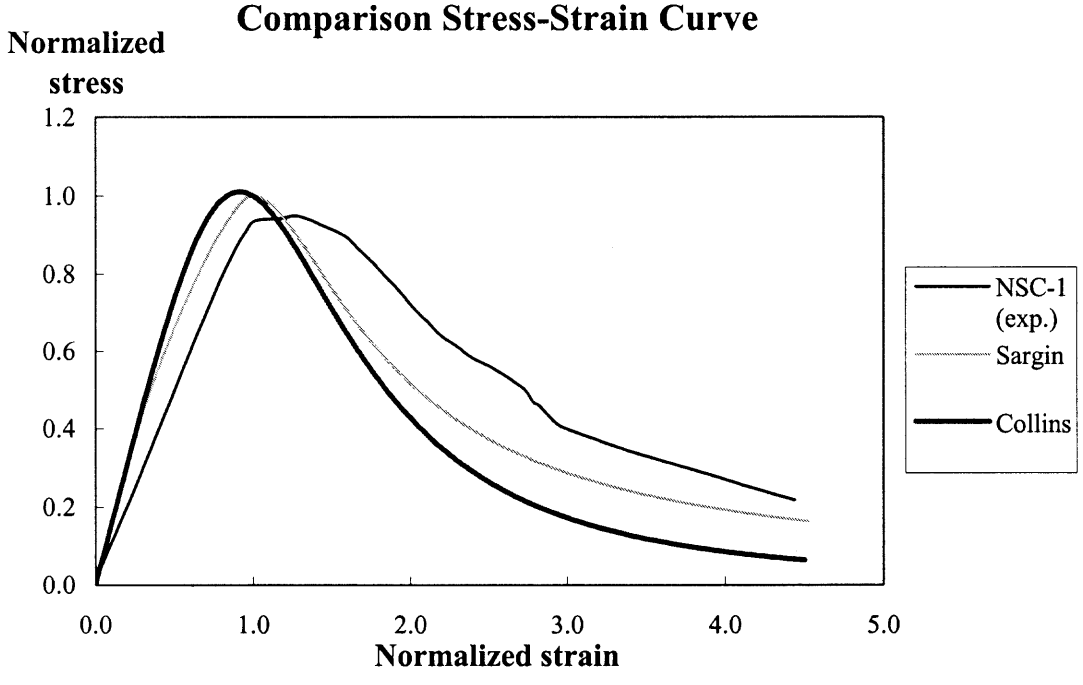

Figure 4.7 Stress-Strain curve of mix NSC-1 compared with the curves proposed by Sargin and Collins.

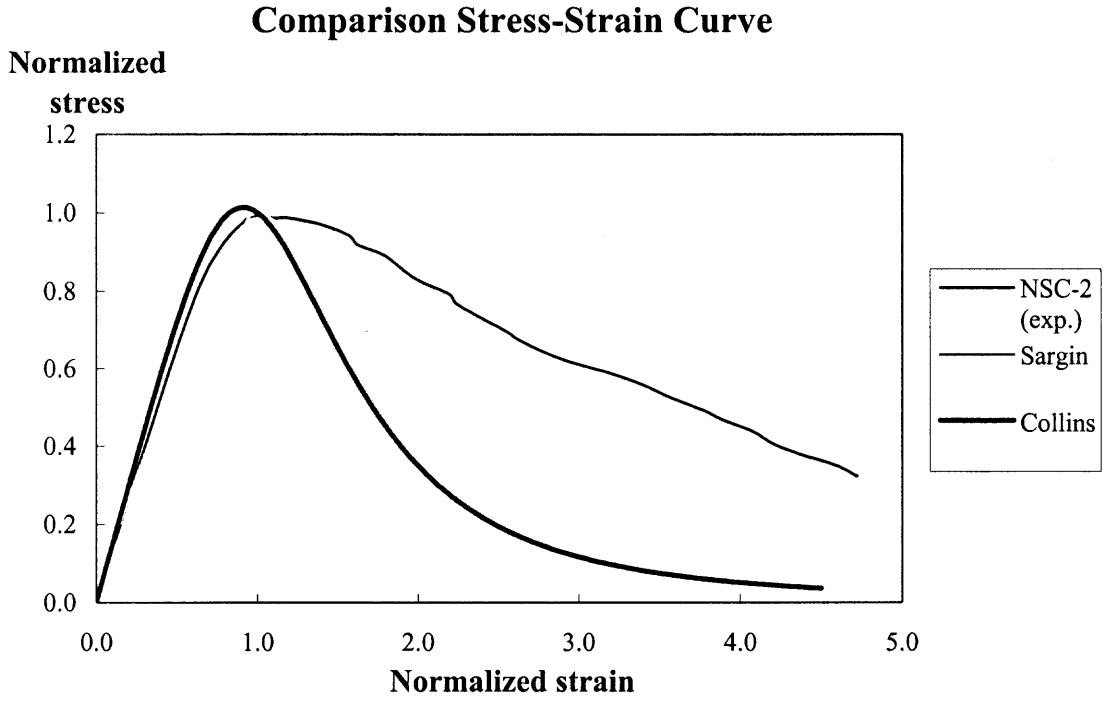

Figure 4.8 Stress-Strain curve of mix NSC-2 compared with the curves proposed by Sargin and Collins.

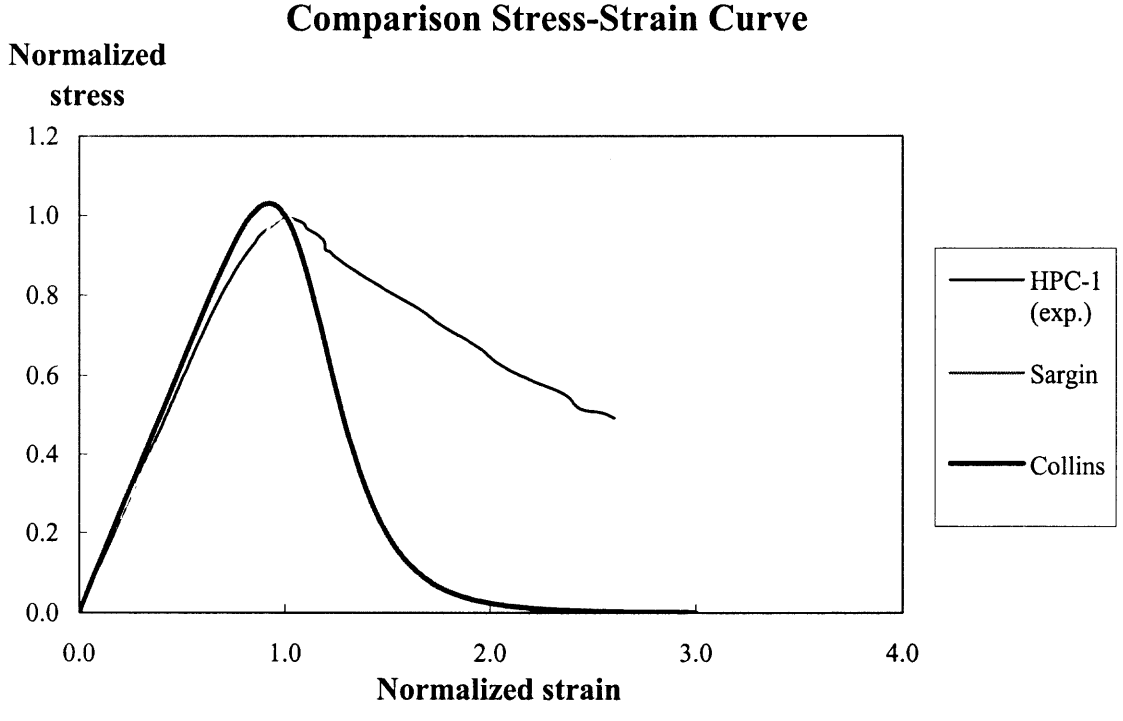

Figure 4.9 Stress-Strain curve of mix HPC-1 compared with the curves proposed by Sargin and Collins.

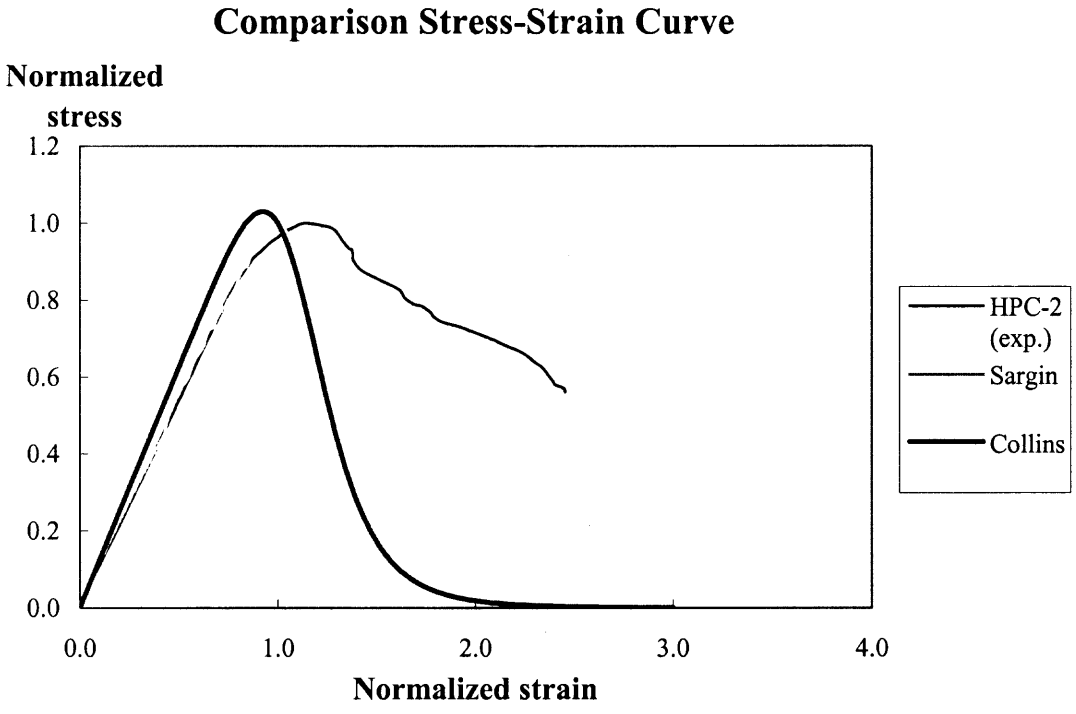

Figure 4.10 Stress-Strain curve of mix HPC-2 compared with the curves proposed by Sargin and Collins.

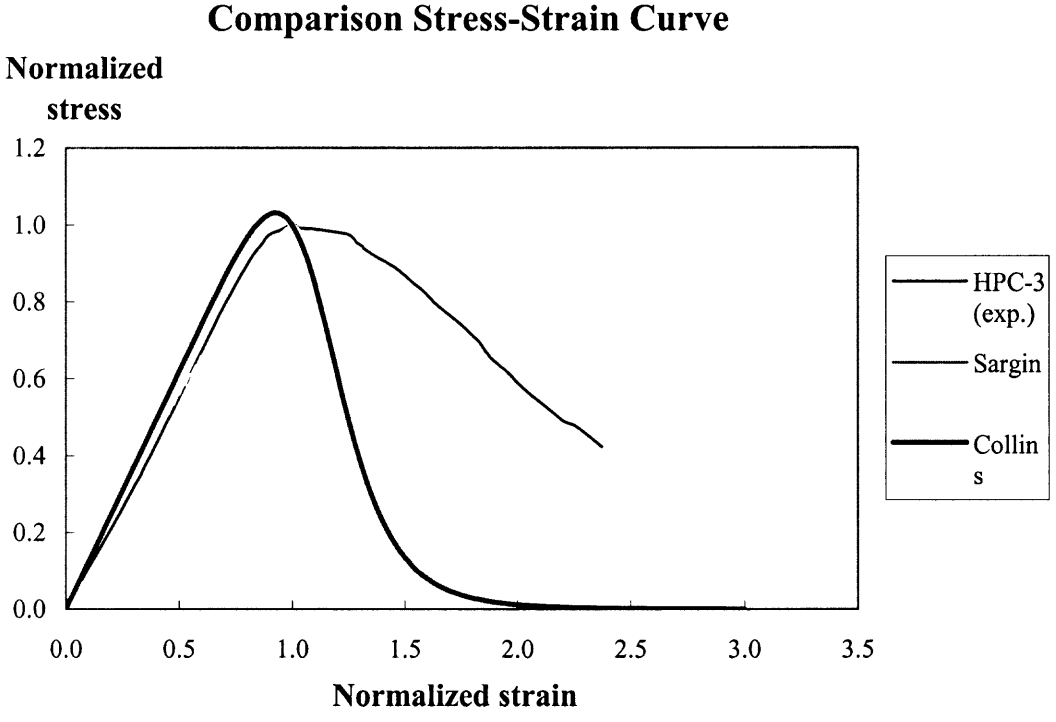

Figure 4.11 Stress-Strain curve of mix HPC-3 compared with the curves proposed by Sargin and Collins

The comparison shows that the equations proposed by Sargin (Adapted by Attard and Setunge) and Collins have similar relationships except the Sargin's equation exhibits more ductility in descending branch (higher compressive stress at the same level of compressive strain). The stress-strain curve obtained in the experiment for both types of concrete exhibit the similar trend when compared to the empirical equations of Sargin and Collins. For the ascending part, both empirical equations applied well with the experimental results while the descending part of the experimental stress-strain curves show a much higher ductility, which can be seen from the much greater stress at the same level of strain. Another way to investigate the difference of the descending part between experimental results and the empirical equations is by observing the slope of the descending part. It can be seen from the comparison of the stress-strain curves that the slope of the descending part of the stress-strain curves obtained from the empirical equations are much steeper as compared to the experimental results. From this observation, it can be concluded that the stress-strain curves obtained from the experiment show higher ductility than that of the stress-strain curves obtained from the empirical equations proposed by Sargin and Collins.

4.3.Cracking Characteristics of Concrete

The mode of failure and cracking characteristics of both types of concrete were observed during the tests. However, it is difficult to study the cracking characteristics at various stages of strain for high performance concrete, especially in the post peak regime, mainly because of the extremely brittle nature of high performance concrete. The high performance concrete specimens usually exploded just passing the peak stress. To avoid

this occurrence, a very slow strain rate ($5x10^{-8}$ to $7x10^{-7}$ in/in/sec) was used, so that it was possible to obtain a gradual failure for HPC cylinders. Fig. 4.12 and Fig. 4.13 show the modes of failure for normal and high performance concrete respectively.

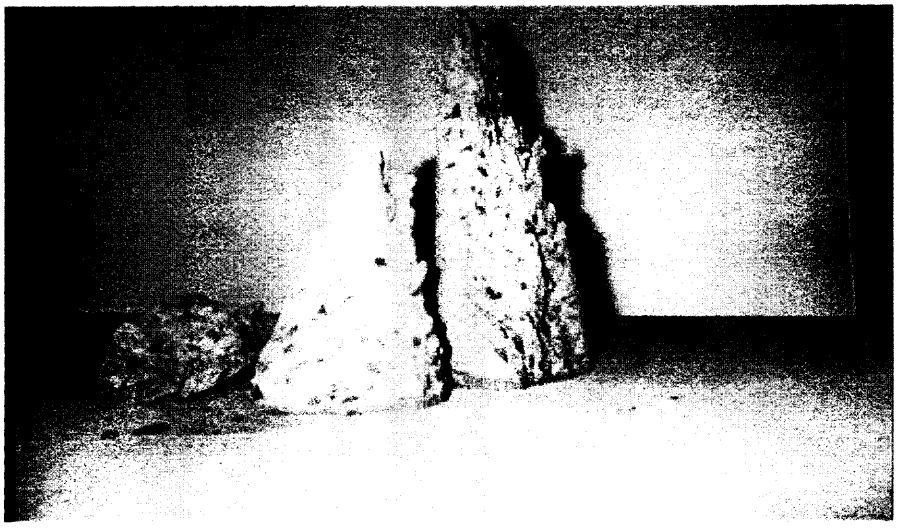

Figure 4.12 Mode of failure of normal strength concrete.

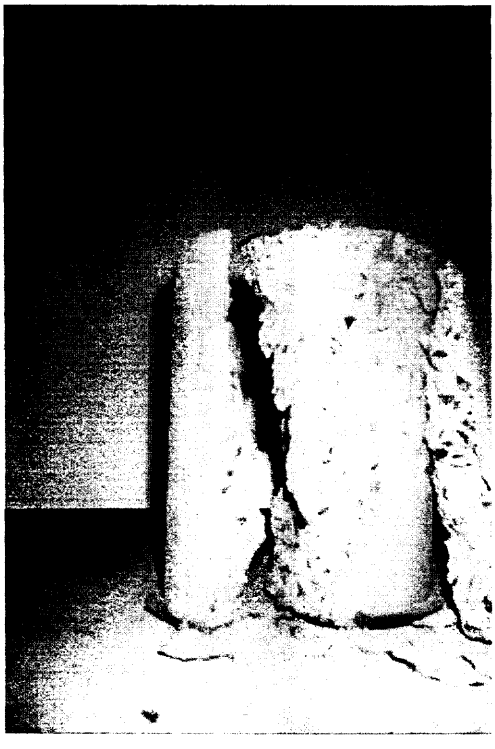

Figure 4.13 Mode of failure of high performance concrete.

The failure mode of normal strength concrete cylinders is different from that of high performance concrete. The crack surfaces of NSC generally develop between the interface of aggregate and the cement paste, cracking shape of the specimens looked like a cone-shape as a result of the combination of shear failure and tensile splitting. On the other hand, cracking in HPC is more localized, the number and length of continuous crack patterns developed at failure are smaller than those of NSC. This seems to imply that the failure mode of HPC cylinders in compression is typical of that of nearly homogeneous material: failure occurs suddenly in vertical, nearly flat plane passing through the coarse aggregate and mortar. This indicates that the strength of the cement-matrix is higher than that of the aggregate. Therefore, the strength of the coarse aggregate becomes one of the controlling factors for the ultimate strength of high performance concrete. The influence of the coarse aggregate was found to be less important for normal strength concrete.

4.4 Stress-Strain Behavior of Concrete under Cyclic Loading

The complete stress-strain curves of concrete cylinders under cyclic loading were also obtained in this study. To achieve these curves, the specimens were loaded for normal and high strength concrete in strain control mode at very low rates as mentioned in Chapter 3. Comparison of the stress-strain curves between monotonic loading and cyclic loading were shown in Figure 4.14 for normal strength concrete and Figure 4.15 for high performance concrete respectively. It can be seen from the stress-strain curves of both types of concrete that the reloading path of the cyclic responses always join the monotonic stress envelop, almost at the level of previously attained maximum stress.

It can be concluded from the similarity of both the monotonic and the cyclic stress-strain curves that the specimens subjected to unloading and reloading cycles experience very little strength degradation, which suggests that the strength criteria for concrete are basically path-independent.

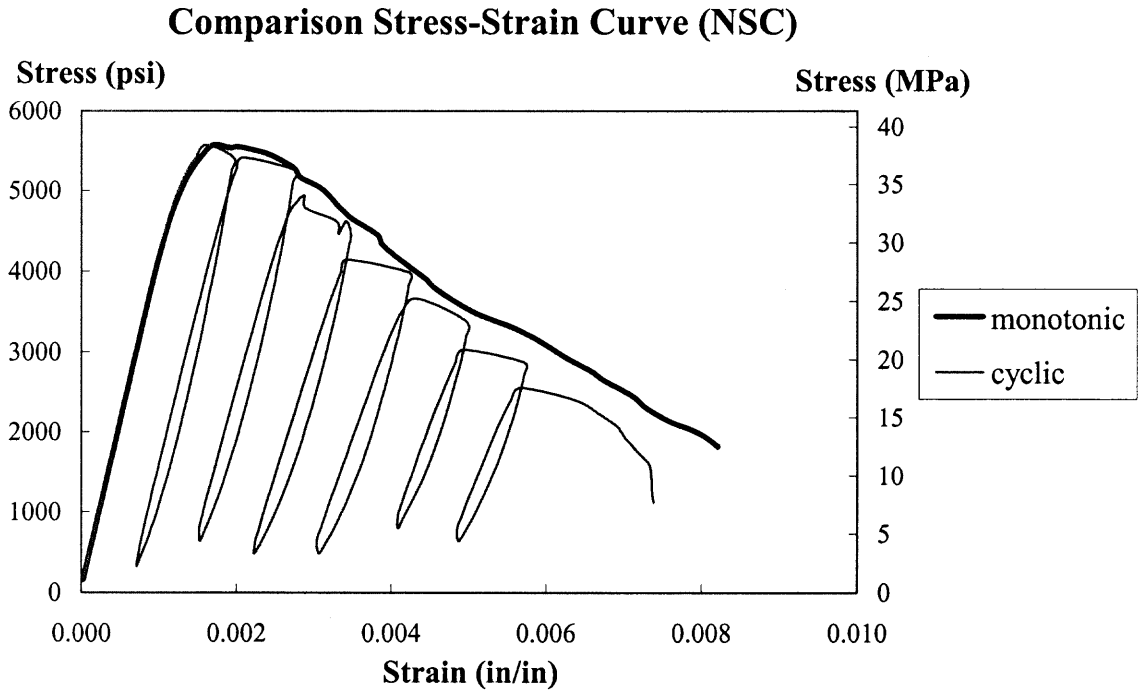

Figure 4.14 Comparison of stress-strain curve between monotonic loading and cyclic loading of normal strength concrete.

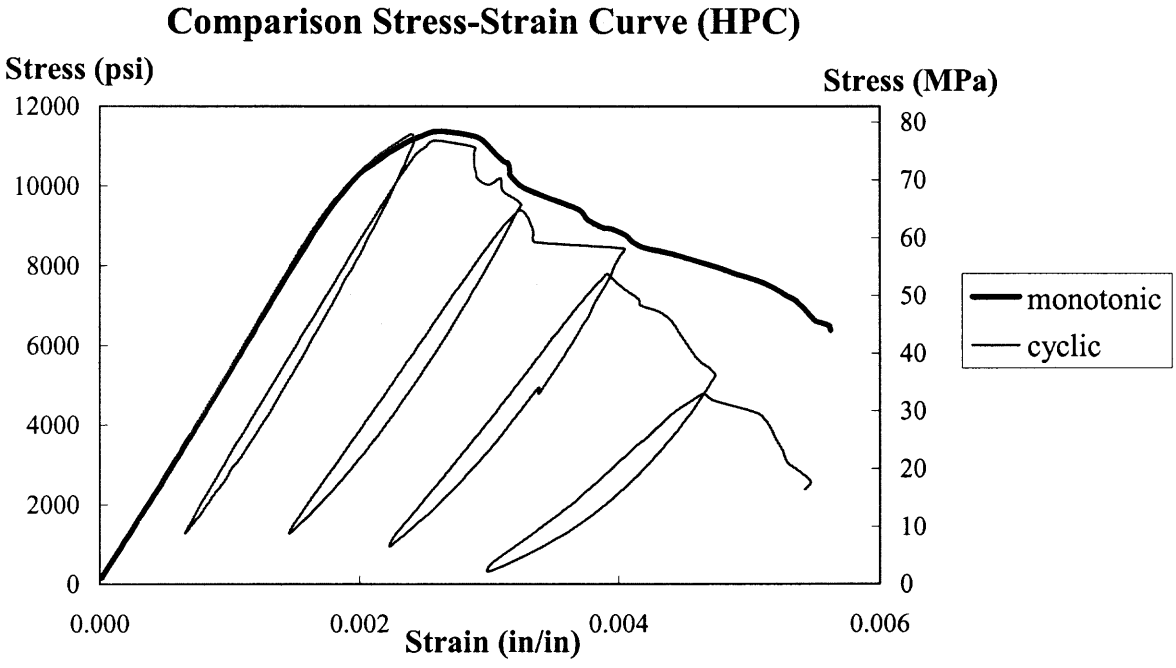

Figure 4.15 Comparison of stress-strain curve between monotonic loading and cyclic loading of high performance concrete.

However, the cyclic stress-strain curves exhibited hysteresis during unloading and reloading cycles, especially in the post-peak stress level of concrete. The magnitude of this hysteresis is a measure of the amount of energy dissipation due to crack formation during the loading cycles. Moreover, the unloading and reloading curves did not coincide and were not parallel to the initial loading curve. The average slope of the unloading and reloading curves is inversely proportional to the plastic strain. This implies that there is a definite stiffness degradation for the entire strain range of stress-strain curve.

The amount of hysteresis was shown to be greater for normal strength concrete, it can be observed from the bigger area between unloading and reloading curves of cyclic stress-strain responses. From this result, we can conclude that normal strength concrete can dissipate energy under loading better than that of high strength concrete. And that is

the reason why normal strength has the higher number and length of continuous crack patterns developed at failure than those of high strength concrete. It was also observed from the cyclic stress-strain curves that the average slope of the unloading and reloading curve of the two successive cycles decreased in a greater degree for normal strength concrete, which means normal strength concrete has more stiffness degradation than that of high strength concrete, especially in the post-peak regime.

CHAPTER 5

CONCLUSION

From the experimental results obtained throughout the course of this study, the following conclusions can be drawn as follows:

1. In the uniaxial compression experiment of concrete cylinders, the results show that the strain at peak stress of normal strength concrete is usually less than that of high performance concrete, modulus of elasticity of high performance concrete is higher than that of normal strength concrete, and Poisson's ratio of high performance concrete is less than that of normal strength concrete. (The average Poisson's ratio is 0.183 for HPC and 0.205 for NSC.) The equations for predicting the modulus of elasticity provided by ACI 318-99 and ACI 363-88 are applicable for the test results of normal strength concrete, while the equation from ACI 318-99 tends to overestimate the modulus of elasticity of high performance concrete.

2. For high performance concrete, the shape of the ascending part of the stress-strain curve is more linear and steep. The slope of the descending part is also steeper as compared to normal strength concrete because of a decrease in the extent of internal microcracking occurred in higher strength concrete.

3. Normal strength concrete has a higher ductility ratio than that of high performance concrete. It can be concluded that normal strength concrete has more ability to sustain large inelastic deformation without substantial reduction in strength and also more ability to absorb and dissipate seismic energy through relative stable hysteresis loops. However, ductility of high performance concrete can be increased by using steel reinforcements, mostly in the form of lateral confinements such as in columns.

4. The stress-strain curves obtained in the experiment for both types of concrete exhibit a similar trend when compared to the empirical equations of Sargin and Collins. For the ascending part, both empirical equations can be applied to the experimental results, while the descending part of the experimental stress-strain curves shows much higher ductility. It can be seen from the comparison of stress-strain curves that the slopes of the descending part of the stress-strain curves obtained from the empirical equations are much steeper as compared to the slopes obtained from the experiment.

5. The crack surfaces of normal strength concrete generally develop between the interface of aggregate and the cement paste. On the other hand, cracking in high performance concrete is more localized, and the number and length of continuous crack patterns developed at failure are smaller than those of normal strength concrete. For this reason, the failure mode of high performance concrete is typical of that of nearly homogeneous material. In addition, the strength of the coarse aggregate was found to be the controlling factor for the ultimate strength of high performance concrete. The influence of coarse aggregate is found to be less important for normal strength concrete.

6. In the cyclic-loading test, it can be seen from the stress-strain curves of both types of concrete that the reloading path of the cyclic responses always joins the monotonic stress envelops. That means that specimens subjected to unloading and reloading cycles experience very little strength degradation, which suggests that the strength criteria for concrete are basically path-independent.

7. The amount of hysteresis during unloading and reloading cycles was shown to be greater for normal strength concrete. It indicates that normal strength concrete has more ability to dissipate energy under loading than that of high performance concrete. It was

also observed from the cyclic stress-strain curves that the average slope of the unloading and reloading curves of two successive cycles decreases in greater degree for normal strength concrete, which means normal strength concrete has more stiffness degradation than that of high performance concrete, especially in the post-peak regime.

REFERENCES

1. ACI Committee 363, "State-of-the-Art Report on High Strength Concrete," *ACI Journal*, vol. 81, no. 4, pp. 364-411, July-August, 1984.

2. A. Guerrero, S. Goni, A. Macias, and M. P. Luxan, "Effect of the starting fly ash on the microstructure and mechanical properties of fly ash-belite cement mortars," *Cement and Concrete Research*, vol. 30, pp. 553-559, 2000.

3. A. P. Boresi, O. M. Sidebottom, F. B. Seely, and J. O. Smith, *Advanced Mechanics of Materials*, John Wiley and Sons, New York, third ed., 1978.

4. A. Peled, M. F. Cyr, and S. P. Shah, "High content of fly ash (Class F) in extruded cementitious composites," *ACI Materials Journal*, Title no. 97-M59, pp. 509-517.

5. ASTM C39-96, "Standard test method for compressive strength of cylindrical concrete specimens," *ASTM Standards*, vol. 04.02, 1999.

6. ASTM C192/C, 192/M-98, "Standard practice for making and curing concrete test specimens in the laboratory," *ASTM Standards*, vol. 04.02, 1999.

7. ASTM C311-98b, "Standard test methods for sampling and testing fly ash or natural pozzolans for use as a mineral admixture in Portland-cement concrete," *ASTM Standards*, vol. 04.02, 1999.

8. ASTM C617-98, "Standard practice for capping cylindrical concrete specimens," *ASTM Standards*, vol. 04.02, 1999.

9. ASTM C618-98, "Standard specification for coal fly ash and raw or calcined natural pozzolan for use as a mineral admixture in concrete," *ASTM Standards*, vol. 04.02, 1999.

10. C. K. Wang and C. G. Salmon, *Reinforced Concrete Design*, Harper & Row Publishers, third edition, pp. 3-5, 1979.

11. C. S. Poon, L. Lam, and Y. L.Wong, "A study on high strength concrete prepared with large volumes of low calcium fly ash," *Cement and Concrete Research*, vol. 30, pp. 447-455, 2000.

12. D. P. Candappa, S. Setunge, and J. G. Sanjayan, "Stress versus strain relationship of high strength concrete under high lateral confinement," *Cement and Concrete Research*, vol. 29, pp. 1977-1982, 1999.

13. E. E. Berry, "Fly Ash Use in Concrete Part 1," *A critical review of the chemical, physical, and puzzolanic properties of fly ash*, CANMET REPORT, pp. 76-25, 1976.

14. F. DeLarrard, J. M. Torrenti, and P. Rossi, "Le flambement a deux echelles dans la rupture du be'tons en compression," *Bulletin de liaison des Laboratoires des Ponts et. Chauaae 'es*, pp. 51-55, March-April, 1988.

15. F. D. Lydon, *Concrete Mix Design*, Applied Science Publishers Ltd., London, 1979.

16. F. J. Young, "Very High Strength Cement-Based Materials," *Symposia proceedings*, vol. 42, Materials Research Society, Pittsburgh, 1985.

17. G. Penelis and A. J. Kappos, *Earthquake-Resistant Concrete Structures*, E & FN SPON, first edition, Great Britain, 1997.

18. G. R. White, *Concrete Technology*, Delmar Publisher Inc., New York, third ed., 1991.

19. Hashin, "The moduli of heterogeneous materials," *Journal of Applied Mechanics*, March, 1962.

20. J. C. McCormac, *Design of Reinforced Concrete*, Harper & Row Publishers Inc., second edition, pp. 1-6, 1986.

21. J. M. Mander, M. N. Priestly, and R. Park, "Theoretical Stress-Strain Model for Confined Concrete," *Journal of Structural Division*, ASCE, vol. 114, no. 8, pp. 1804-1826, 1988.

22. K. Billig, *Structural Concrete*, Macmillan & Co Ltd., pp. 3-5, London, 1960.

23. K. K. B. Dahl, "Uniaxial Stress-Strain Curves for Normal and High Strength Concrete," *ABK Report no. R282*, Department of Structural Engineering, Technical University of Denmark, 1992.

24. K. Wesche, *Fly ash in concrete : Properties and Performance*, Rilem report 7, Chapman and Hall, London, 1991.

25. M. D. A. Thomas, M. H. Shehata, and S. G. Shashiprakash, "The use of fly ash in concrete : classification by composition," *Cement Concrete and Aggregates*, vol. 21, no. 2, pp. 105-110, Dec. 1999.

26. M. I. Khan, C. J. Lynsdale, and P. Waldron, "Porosity and strength of PFA/SF/OPC ternary blended paste," *Cement and Concrete Research*, vol. 30, pp. 1225-1229, 2000.

27. M. M. Attard and S. Setunge, "Stress-Strain Relationship of Confined and Unconfined Concrete," *ACI Materials Journal*, vol. 93, no. 5, pp. 432-442, September-October, 1996.

28. M. P. Collins, D. Mitchell, and J. G. MacGreger, "Structural Design Considerations for High Strength Concrete," *Concrete International*, pp. 27-34, May, 1993.

29. M. Regourd, B. Mortureux, P. C. Aitcin, and P. Pinsonneuult, "Microstructure of field concretes containing silica fume," *4th International Conference on Cement Microscopy*, Las Vegas, pp. 249-260, April, 1982.

30. M. Regourd-Moranville, "Microstructures des b'etons a hautes performances," *Formation Continue ENPC*, March, 1989.

31. M. Sargin, "Stress-Strain Relationship for Concrete and the Analysis of Structural Concrete Sections," *Study No.4*, Solid Mechanics Division, University of Waterloo, Ontario, p. 167, 1971.

32. M. Wecharatana and J. W. Liskowitz, "Properties of High Performance Fly Ash Concrete," *International Workshop on High Performance Concrete*, Bangkok, Thailand, pp. 28-1 to 28-2, Nov. 21-22, 1994.

33. M. Wecharatana, R. K. Navalurkar, C. T. Hsu, and S. K. Kim, "True Fracture Energy of Concrete," *ACI Materials Journal*, vol. 96, no. 2, pp. 213-224, March-April, 1999.

34. P. M. Nielson, J. Christoffersen, and J. Frederiksen, "Danish high performance concretes," *International Workshop on High Performance Concrete*, Bangkok, Thailand, pp. 11-1 to 11-12, Nov. 21-22, 1994.

35. P. T. Wang, S. P. Shah, and A. E. Naaman, "Stress-Strain Curves of Normal and Lightweight Concrete in Compression," *ACI Materials Journal*, vol. 75, no. 11, pp. 603-611, November-December, 1978.

36. S. P. Timoshenko and J. M. Gere, *Mechanics of Materials*, Van Nostrand Reinhold Company, New York, 1972.

37. S. Popovics, "A Review of Stress-Strain Curve of Concrete," *Cement and Concrete Research*, vol. 3, no. 4, pp. 583-599, September, 1973.

38. S. Setunge, "Structural Properties of Very High Strength Concrete," *Ph.D. Thesis*, Monash University, 1993.

39. T. L. Carrasquillo, F. O. Slate, and A. H. Nilson, "Microcracking and Behavior of High Strength Concrete subjected to Short Term Loading," *ACI Materials Journal*, vol. 78, no. 3, pp. 171-178, 1981.

40. V. Mier, "Complete Stress-Strain Behavior and Damaging Status of Concrete under Multiaxial Conditions," *RILEM-CEB-CNRS*, International Conference on Concrete under Multiaxial Conditions, vol. 1, Presses de l'Universite Paul Sabatier, Toulouse, France, 1984.

41. V. W. Berg, "Kostenorientierter Betonentwurf Fuer Flugaschehaltige Betone," *Betonwerk und Fertigteiltechnik 47*, pp. 401-407, 1981.

42. W. T. Hester, "High-Strength Concrete," *Second International Symposium*, ACI SP-121, Detroit, 1990.

43. Y. Malier, *High Performance Concrete : From Material to Structure*, E & FN SPON, London, 1992.